

6L02151

# Interpretation of Gravity Data in a Complex Volcano-Tectonic Setting, Southwestern Nevada

DAVID B. SNYDER<sup>1</sup>

*U.S. Geological Survey, Menlo Park, California*

W. J. CARR

*U.S. Geological Survey, Denver, Colorado*

This regional gravity study, based on an irregular 2-km data grid, was conducted during the past few years at Yucca Mountain, southern Nye County, Nevada, as part of a program to locate a suitable repository for high-level nuclear waste. About 100 surface rock samples, three borehole gamma-gamma logs, and one borehole gravity study provide excellent density control. A nearly linear increase in density of 0.26 g/cm<sup>3</sup> per kilometer of depth is indicated in the thick tuff sequences that underlie the mountain. Isostatic and 2.0-g/cm<sup>3</sup> Bouguer corrections were applied to the observed gravity values to remove regional gradients and topographic effects, respectively. The Bare Mountain gravity high, with an isostatic anomaly maximum of 48 mGal, is connected with a greater gravity high over the Funeral Mountains, to the southwest; together, these highs result from a continuous block of dense, metamorphosed Precambrian and Paleozoic rocks that stretches across much of the Walker Lane from the east edge of Death Valley to Bare Mountain. The Calico Hills gravity high appears more likely to originate from a northeast trending buried ridge of Paleozoic rocks that extends southwestward beneath Busted Butte, 5 km southeast of the proposed repository, where two- and three-dimensional modeling indicates that the pre-Cenozoic rocks lie less than 1000 m beneath the surface. Tuff, at least 4000 m thick, fills a large steep-sided depression in the pretuff rocks beneath Yucca Mountain and Crater Flat. The gravity low and the thick tuff section lie within a large collapse area that includes the Crater Flat-Timber Mountain-Silent Canyon caldera complexes. Gravity lows in Crater Flat itself are interpreted to coincide with the source areas of the Prow Pass Member, the Bullfrog Member, and the Tram Member of the Crater Flat Tuff; these source areas add nearly 350 km<sup>2</sup> to the previously recognized extent of the local caldera complexes. Southward extension of the broad gravity low associated with Crater Flat into the Amargosa Desert is evidence for sector graben-type collapse segments related to the formation of the Timber Mountain caldera and superimposed on the other volcanic and extensional structures within Crater Flat.

## INTRODUCTION

This gravity study is concentrated in southwest Nevada near the California border and Death Valley (Figure 1) and on the southwest side of the southwestern Nevada volcanic field (Figure 2a). This volcanic field includes the Timber Mountain caldera complex [Byers *et al.*, 1976] and the Crater Flat-Prospector Pass caldera complex [Carr *et al.*, 1984], the sources of numerous, voluminous eruptions from about 16 to 10 Ma ago. A general understanding of the near-surface structure of this volcanic field has existed for more than a decade. In the last few years and as a result of exploration at Yucca Mountain for a repository to hold high-level nuclear waste, geologic and geophysical studies have outlined the complex crustal structures and tectonic history of the region in greater detail.

Gravity investigations play an important role in the characterization of Yucca Mountain as a possible nuclear waste repository. In and near the mountain Cenozoic sedimentary and volcanic rocks obscure the more complex pre-Tertiary geology, and therefore obtaining information about subsurface rock geometry is critical to fully characterize the water flow patterns in the area. The candidate repository site (Figure 1) lies within tuff composing the northern part of Yucca Mountain, a relatively coherent block of rocks within a stratigraphically and structurally complex region. This study

explores and interprets the three-dimensional structure and geometry of the rocks surrounding the candidate site; it updates a preliminary report [Snyder and Carr, 1982] and earlier work by Healey and Miller [1971].

Numerous deep (750-1830 m) holes have been drilled at Yucca Mountain; most have a full suite of geophysical logs. All but three of the holes (Figure 1) are in or near the candidate site area and include USW-G1 [Spengler *et al.*, 1981], USW-G2 [Maldonado and Koether, 1983], USW-G3, UE25P-1, and USW-H1. Other holes drilled a little farther outside the site area include J-13 near Fortymile Wash, UE25a-3 in the Calico Hills [Maldonado *et al.*, 1979], and USW-VH-1 [Carr, 1982] and USW-VH-2 in Crater Flat. Geologic, geophysical, and hydrologic data have been obtained from these holes, and this information has been used both directly and indirectly in interpreting the structure of the area. Drill holes UE25a-3 and UE25P-1 reached pre-Tertiary rocks, at depths of 1 and 1240 m, respectively, but several holes in the area (G1, G2, G3, and H1) were drilled to depths of about 1830 m without reaching the base of the volcanic rocks (Figure 3). Alteration was especially notable in the lower part of the section penetrated by these deep holes [Waters and Carroll, 1981], and metamorphic effects, including density change, increase steadily downward.

Four aeromagnetic surveys are encompassed by the area of the gravity study. Constant-barometric-elevation surveys [Boynton and Vargo, 1963; U.S. Geological Survey, 1971], flown at 2440 and 2740 m, respectively, indicate a strong gradient across northern Yucca Mountain that increases in total intensity to the north. The breadth and slope of this gradient suggest that the source lies at a minimum depth of

<sup>1</sup>Now at Department of Geological Sciences, Cornell University.

This paper is not subject to U.S. copyright. Published in 1984 by the American Geophysical Union.

Paper number 4B0782.

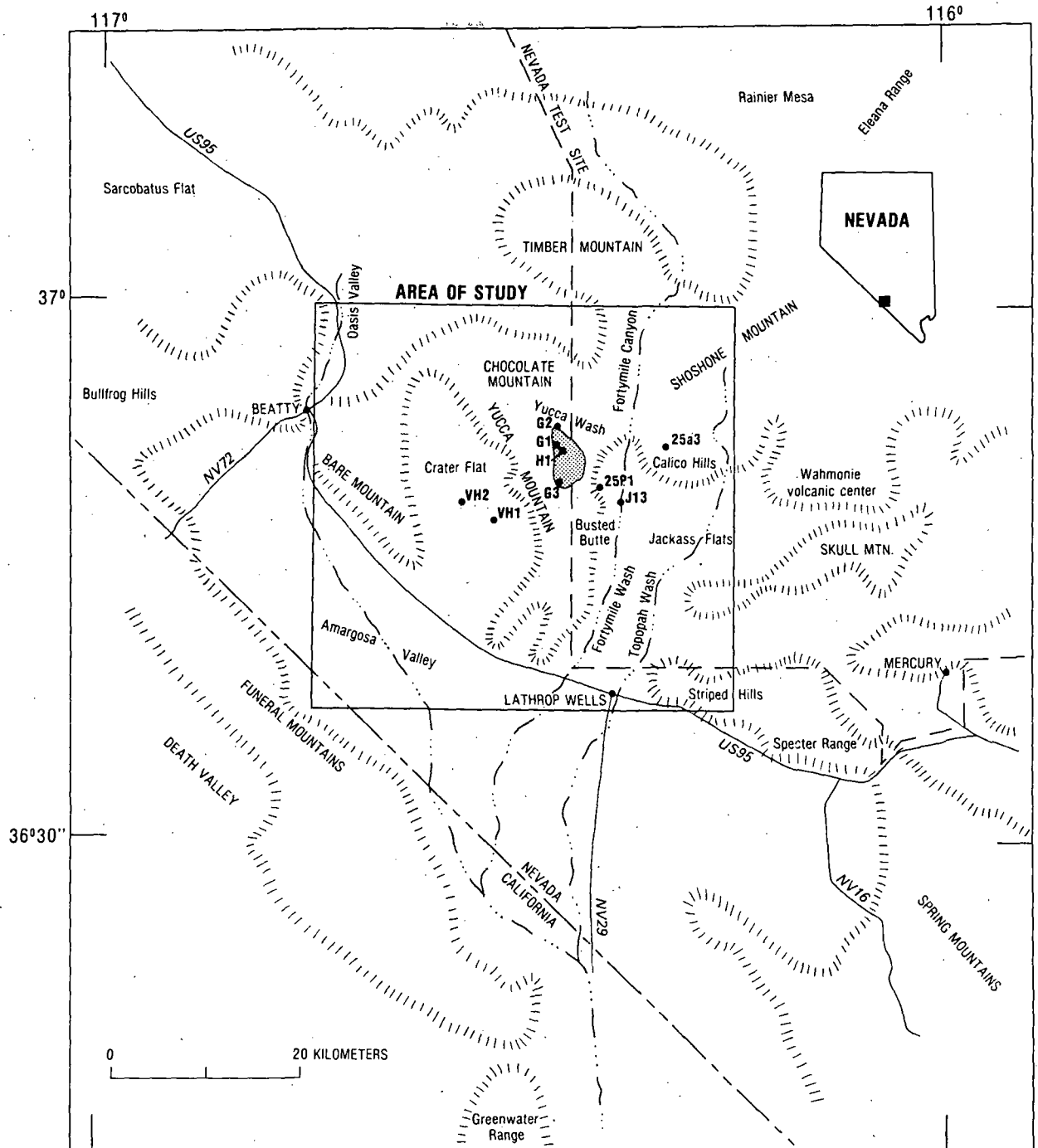


Fig. 1. Index maps showing location of study area (also area of Figures 2 and 4), local physiography, and cultural landmarks. Shaded area represents the potential repository site area. Numbers, such as G1, represent drill hole locations; the USW and UE prefixes of the full designations have been omitted for simplicity.

2200 m (G. D. Bath, written communication, 1980). Two later surveys, flown at constant terrain clearance of 120 m, also covered the study area [U.S. Geological Survey, 1978, 1979].

Seismic and electrical techniques thus far have been only partly successful; no clear characterization of the rocks below 500 m has been obtained as yet by these methods. Seismic refraction experiments are testing the gravity model presented here [Mooney *et al.*, 1982]; one unreversed east-west profile produced a velocity cross section compatible with the gravity model and indicated additional structures within the Precambrian and Paleozoic rocks at depths greater than the resolution range of the gravity study.

#### GEOLOGY OF YUCCA MOUNTAIN AND VICINITY

Yucca Mountain lies in the southern part of the Great Basin section of the Basin and Range physiographic province and within the Walker Lane [Locke *et al.*, 1940; Carr, 1974]. Much of the Great Basin is characterized by typical basin-and-range topography, with alternating north trending ridges and valleys. The Walker Lane exhibits more diverse topography of generally lower relief and, locally, arcuate mountain trends; it has been described as a belt of sigmoidal bending and right-lateral faulting [Albers, 1967]. The area around Yucca Mountain shows even less relief than most of the

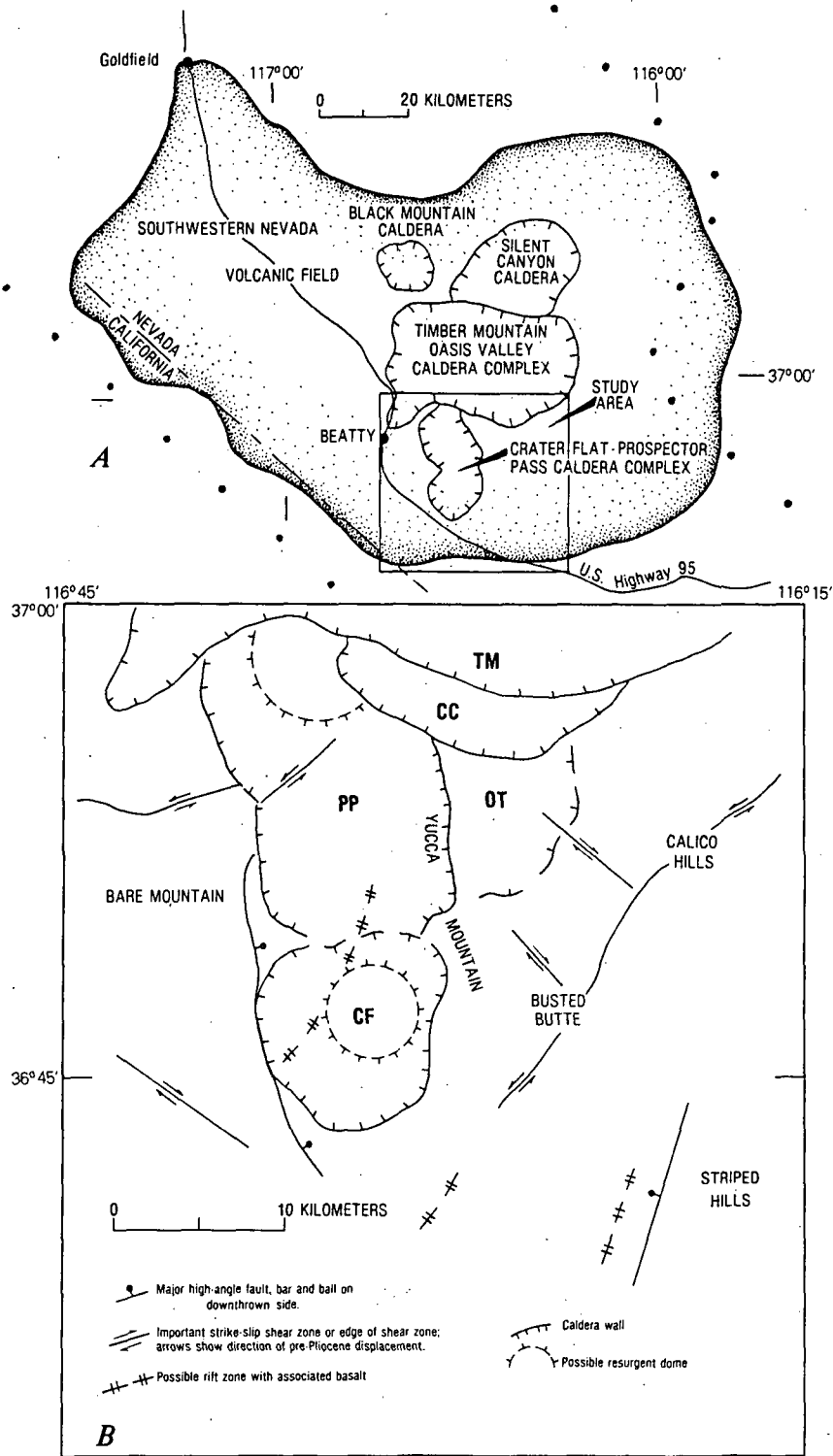


Fig. 2. (a) Map of the southwestern Nevada volcanic field and its component calderas. Dotted lines denote approximate boundary of the Walker Lane. (b) Tectonic-structural diagram of the study area. The location and size of the diagram is indicated by the rectangle in Figures 1 and 2a. Letters identify volcanic structures: TM, Timber Mountain-Oasis Valley caldera complex; CC, Claim Canyon caldera segment; CF, caldera associated with the Bullfrog Member and Prow Pass Member of the Crater Flat Tuff; OT, possible collapse feature filled by older tuff; PP, Prospector Pass caldera segment associated with the Tram Member of the Crater Flat Tuff. Many caldera walls are located with the aid of gravity interpretation.

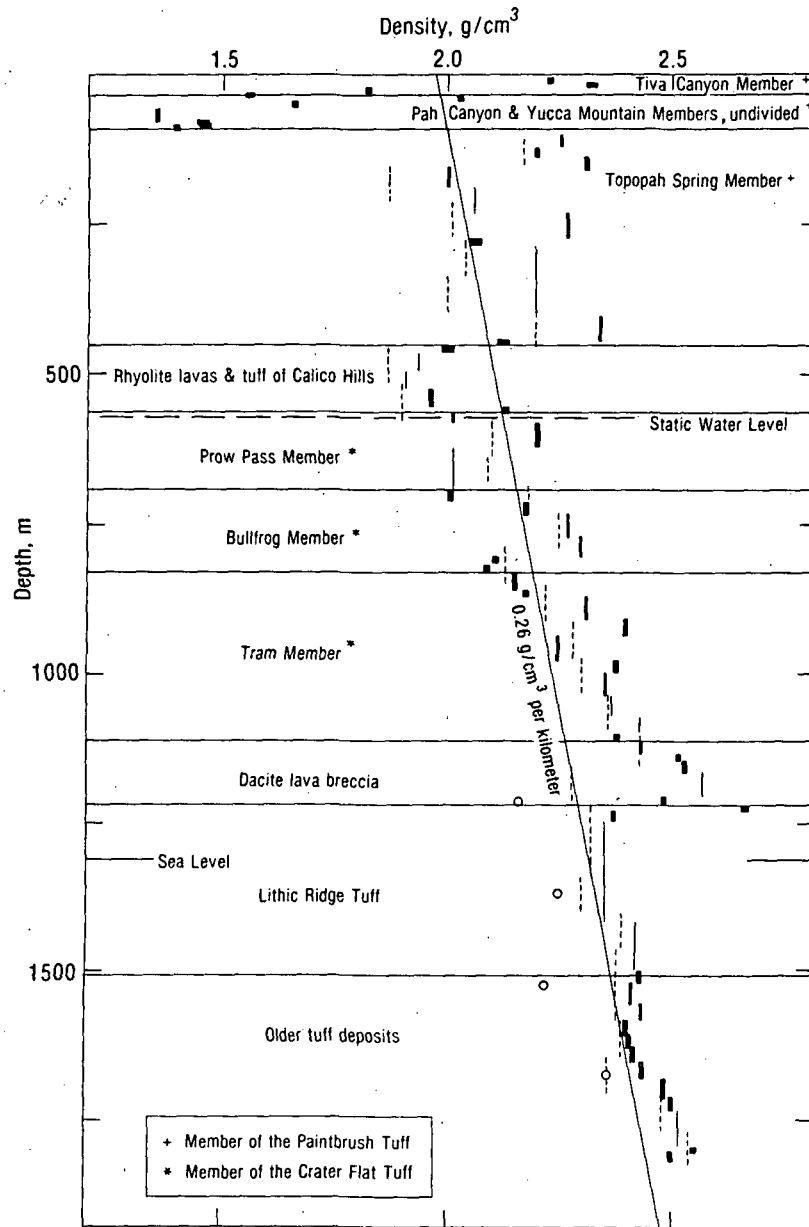


Fig. 3. Density versus depth plot for Tertiary tuff sequence in drill hole USW-H1. Solid rectangles indicate borehole gravity meter determination, depth range, and estimated error range; dashed lines are averaged gamma-gamma log values; circles indicate density measurements of unsaturated drill core obtained from the saturated zone in Yucca Mountain (Table 2). Solid line is least squares fit of the data.

Walker Lane; the characteristic arcuate ranges become less prominent near Yucca Mountain, and broad areas of generally low relief, the Amargosa Desert and Jackass Flats, lie nearby. Yucca Mountain projects into this broad plain from the higher terrain surrounding Timber Mountain (Figure 1) to the north.

#### Stratigraphy

Table 1 is a simplified stratigraphic column of the geologic units in the Yucca Mountain area pertinent to the gravity study. Pre-Tertiary rocks (Figure 4) consist of upper Precambrian and Cambrian clastic units, lower and middle Paleozoic carbonate rocks, and upper Paleozoic detrital rocks. Locally, these rocks are intruded by Mesozoic or Tertiary granitic plutons. Several ancient structural features and depositional zones of Precambrian and Paleozoic age are thought to cross

this general area [Poole, 1974; Stewart, 1980, pp. 40-52], but in many areas thick volcanic rocks of Tertiary age have covered these older structures and rocks. Although the intrusive bodies that crystallized from the magma feeding the Tertiary extrusions remain mostly concealed, hydrothermal alteration zones [Cornwall and Kleinhampl, 1961], dikes and small plugs, and domical structures [Cornwall and Kleinhampl, 1961; Carr and Quinlivan, 1968; Maldonado et al., 1979] suggest the presence of buried intrusive rocks.

Quartzite and other clastic rocks, which predominate within the upper Precambrian and lowermost Paleozoic assemblage, crop out mainly in the western part of the study area, where they are mildly metamorphosed. A thick sequence of limestone and dolomite of Cambrian through Devonian age crops out mostly on Bare Mountain and in the Striped Hills (Figure 1). Thrust or slide masses of Devonian rocks are also present in

TABLE 1. Density and Thickness of Selected Geologic Units in the Yucca Mountain Area

Age	Unit	Approximate Thickness, m	Average Density, g/cm <sup>3</sup>
Quaternary and Tertiary	alluvium	0-300	1.6-2.0
Tertiary	basalt	0-200	2.9
	rhyolite lava flows of Shoshone Mountain	0-100	2.2
	rhyolite lava flows of Fortymile Canyon	0-200	2.2
11.3 Ma*	Timber Mountain Tuff		
	Ammonia Tanks Member and Rainier Mesa Member, undivided	0-150	1.9
12.6 Ma*	Paintbrush Tuff		
	Tiva Canyon Member	120	2.1
	Yucca Mountain Member	0-60	1.9
	Pah Canyon Member	0-70	1.9
13.1 Ma*	Topopah Spring Member	300	2.2
13.4 Ma*	rhyolite lavas and tuff of Calico Hills	10-200	1.9
	Crater Flat Tuff		
	Prow Pass Member	100	2.1
14.0 Ma*	Bullfrog Member	150	2.1
	Tram Member	300	2.25
	rhyodacitic lavas	0-200	2.35
	Lithic Ridge Tuff	300	2.35
	ash flow and bedded tuff	300+	2.45
Tertiary and Mesozoic	granitic intrusive rocks	unknown	2.4?
Late Paleozoic	Tippipah Limestone, Eleana Formation	2000	2.62
	Devils Gate Limestone, Ely Springs Dolomite, Eureka		
Middle and early Paleozoic	Quartzite, Pogonip Group, Nopah Formation, Bonanza King Formation	4000	2.72
	Carrara Formation, Zabriskie		
Early Paleozoic and Precambrian	Quartzite, Wood Canyon Formation, Stirling Quartzite, Johnnie Formation	3500+	2.65

\*Radiometric ages from *Marvin et al.* [1970].

the Calico Hills. Mississippian and Pennsylvanian rocks, principally argillite, quartzite, and limestone, form the lower plate of low-angle faults from Bare Mountain to the Calico Hills and northeastward through the Eleana Range (Figure 1).

Granite crops out at only one locality within the study area. An altered east-west trending granite dike occurs near Beatty at the northwest end of Bare Mountain (Figure 1); a zircon fission track age of  $25.4 \pm 1.3$  Ma (C. W. Naeser, unpublished data, 1983) and geologic relations suggest that the dike is older than known Tertiary volcanism in the region. Granite of Mesozoic age occurs at several localities in the northern part of the Nevada Test Site, and granodiorite of Tertiary age crops out at the Wahmonie volcanic center, just east of the study area [Ekren and Sargent, 1965; Ponce, 1981]. The presence of an extensive caldera complex suggests that granitic rocks underlie much of the northern part of the study area.

The exposed Cenozoic stratigraphic sequence of the area has been well studied. Several volcanic centers within and adjacent to the Timber Mountain-Oasis Valley caldera complex [Marvin et al., 1970; Byers et al., 1976] extruded the Cenozoic tuff and lava flows, some of which are listed in Table 1. Potassium-argon dates indicate that most of the tuff was deposited between 15 and 7 Ma ago; however, the oldest units recently encountered in deep drill holes have not been dated. The great thickness of this tuff indicates the close proximity of its sources. The degree of welding and the density of the tuff vary greatly both laterally and vertically.

Alluvium is widespread and thick in Crater Flat, Jackass

Flats, and the Amargosa Valley. The alluvium consists mostly of detritus from weathered and eroded tuff, but adjacent to Bare Mountain and the Striped Hills it contains considerable quartzite and carbonate rock clasts. Locally, caliche cement is conspicuous in the alluvium. Basalt crops out and inter-tongues with the alluvium, principally in southern Crater Flat, around Jackass Flats, and in the moat of the Timber Mountain caldera. The basaltic activity spans most of the alluvial depositional history but has had pulses about 3.75, 1.1, and 0.3 Ma ago [Vaniman et al., 1980].

#### Rock Densities

In the Yucca Mountain area, density data from surface samples are augmented by both gamma-gamma and borehole gravity measurements in several drill holes. This combination of sample and borehole measurements provides a much better constraint on the rock densities than is available in most gravity studies. The densities of six core samples from drill holes USW-G1 and USW-VH-1, and of 95 surface samples, were measured (Table 2).

Surface samples provide the only density control on the lower Paleozoic rocks modeled in this study. Pre-Tertiary rocks beneath Crater Flat, Yucca Mountain, and Jackass Flats have been sampled only by drill hole UE25P-1, and their exact lithology and density remain largely unknown. Drill hole UE25P-1 penetrated middle Paleozoic dolomite at a depth of 1240 m; preliminary density logs from 1240- to 1800-m depths indicate a bulk density of about 2.75 g/cm<sup>3</sup>.

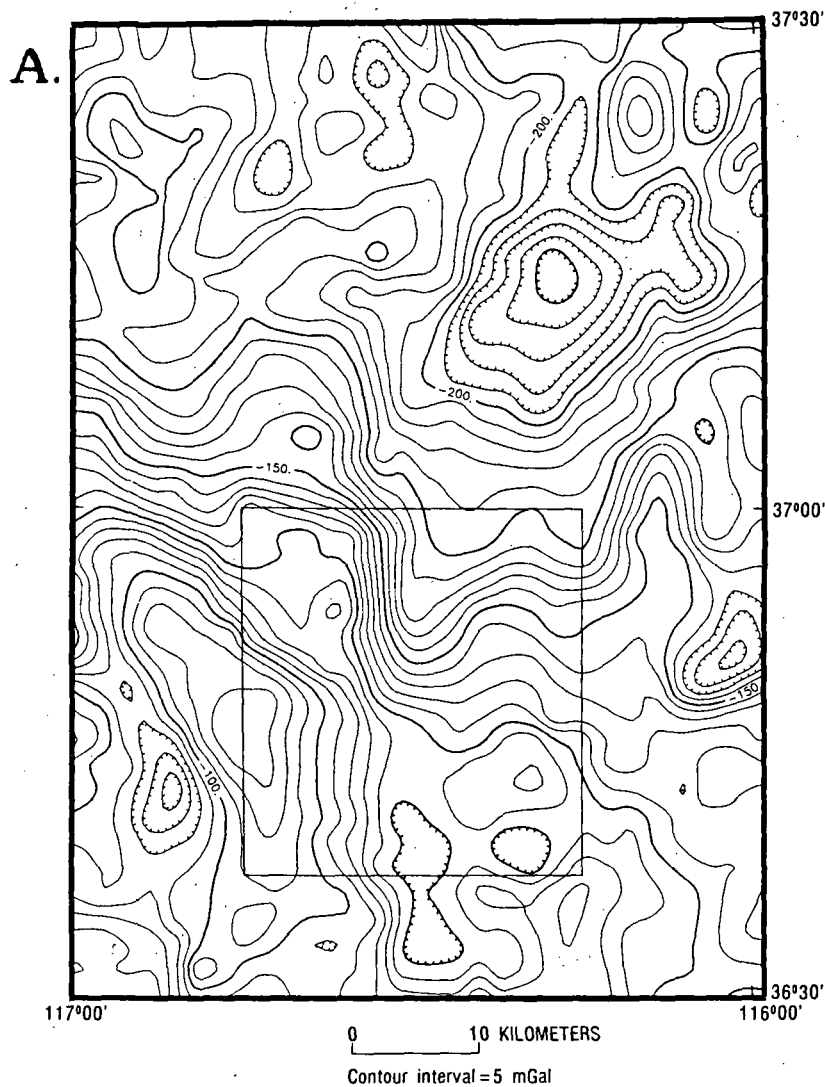


Fig. 4a. Complete Bouguer anomaly map of the region surrounding Yucca Mountain. Area of Figures 4b and 4c is indicated by the rectangle.

The density of saturated pre-Tertiary rock samples ranges from 2.60 to 2.82, with a mean of  $2.66 \pm 0.06$  ( $1\sigma$ )  $\text{g}/\text{cm}^3$ , on the basis of samples taken from outcrops at Bare Mountain and the Striped Hills (Table 2); values in Table 1 are averages of the samples from each rock group listed.

Gamma-gamma density logs were obtained in drill holes USW-G1, H1, and VH-1. These logs have been borehole compensated; that is, any variations in hole diameter caused by wall collapse or the drilling process have been accounted for in the density determinations. The compensated density log curves were then integrated within specified depth intervals to produce an average value for each interval. This analysis further smoothed irregularities caused by fractures in the drill hole walls. The observed downward increase in density (Figure 3) appears to be related to the closing of pore space due to alteration and compaction rather than to primary density variations in the tuff. Nearly linear density increases within individual tuff units (for example, Tram Member in Figure 3) are clearly attributable to the degree of welding and cooling history of the tuff at the time of emplacement.

A downhole gravity study was made in drill hole USW-H1 [Robbins *et al.*, 1982]. Values agree well with the gamma-gamma measurements (Figure 3). This agreement is signifi-

cant, because borehole gravity measurements sample a much greater lateral volume than do the density logs and include fractures, cavities, and other large irregularities in the rock.

The three drill holes with gamma-gamma logs provide excellent constraints on the densities of the Cenozoic tuff, basalt, and alluvium. The linear gradient of  $0.26 \text{ g}/\text{cm}^3$  per kilometer of depth, if it is indeed due to alteration and lithostatic loading, is applicable to all the thick tuff sequences within the study area.

#### Structure

The area of this study is near the axis of the Walker Lane and near the southern margin of the southwestern Nevada volcanic field (Figure 2a; Carr *et al.* [1984]). The nearly linear basins and ranges of central Nevada are interrupted in southwestern Nevada by several northwest striking right-lateral fault zones; these fault zones combine with northeast striking fault zones and structures related to numerous nearby calderas to produce a 50- to 100-km-wide northwest trending zone of diverse topography and structure here included in the Walker Lane [Carr, 1974]. Large-scale drag folds or oroclinal bends [Albers, 1967] are associated with parts of the Walker Lane, but in the study area these structures are obscured by

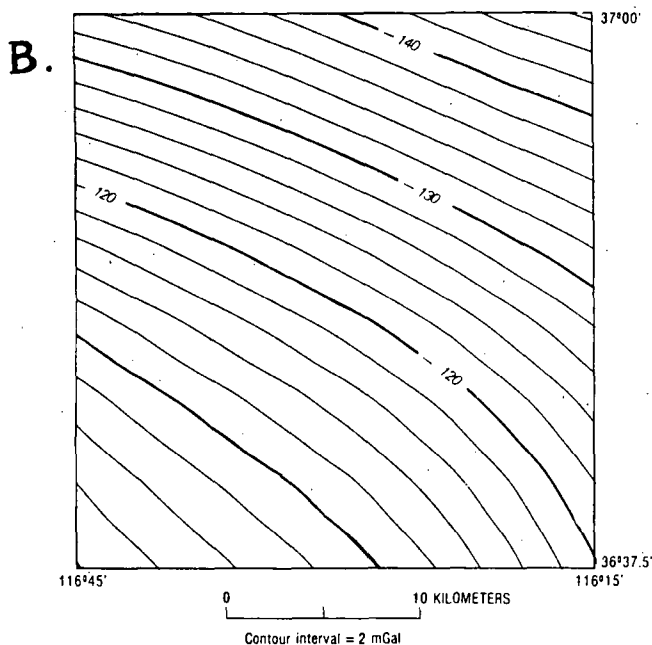


Fig. 4b. Map of isostatic correction applied to the Bouguer anomalies to produce the isostatic residual gravity map. See text for parameters used in the calculation of the correction.

Tertiary volcanic rocks and structures. One exception is Bare Mountain (Figure 4) where large-scale right-lateral drag is observed in the pre-Tertiary rocks. The region was also intruded by east trending Mesozoic granitic plutons while being subjected to crustal shortening caused chiefly by eastward or southeastward directed thrusting and folding [Stewart, 1980]. The study area is also within the Death Valley-Pancake Range belt of Crowe *et al.* [1983], a zone slightly more tectonically active than adjacent areas during latest Miocene to Holocene time. This belt is the locus of basalts less than 8 Ma in age and relatively dense Quaternary faulting [Carr, 1974; Carr and Rogers, 1982, pp. 12-14].

Five main structural elements are recognized within the study area (Figure 2b): (1) the high-standing block of Bare Mountain exposing metamorphism, thrust faults, and folds [Cornwall and Kleinhamp, 1961; Monsen, 1983]; (2) northwest trending valleys, such as the Amargosa Valley and Yucca Wash (Figures 1 and 2b), that represent the location of fault zones of that trend; (3) northeast trending structural zones in the northwest and southeast quadrants of the study area (Figure 2b); (4) north to northeast striking basin-range faults and grabens mostly in the Lathrop Wells area, on Yucca Mountain, and in Crater Flat; and (5) large volcano-tectonic features related to and including the Timber Mountain-Oasis Valley and Crater Flat-Prospector Pass caldera complexes [Carr *et al.*, 1984]. These caldera and collapse features are largely superimposed on, but partly controlled by, the other structural elements.

At Bare Mountain the Late Precambrian and Paleozoic rocks are separated from the Tertiary volcanic rocks by a major fault that dips northward at angles of 10°-20° [Cornwall and Kleinhamp, 1961]. Within the Paleozoic rocks, north striking, east dipping normal faults are slightly older or contemporaneous [Monsen, 1983] with silicic dikes that are about 13.9 Ma old (R. F. Marvin, unpublished data, 1980). Low-angle normal faults or glide blocks on Bare Mountain post-date the north striking dikes and faults.

In nearby areas where Tertiary rocks are relatively thin, fault trends in the Paleozoic rocks are similar or coincident with those in the overlying Tertiary rocks, and the displacements in the Paleozoic rocks are distinctly larger [Sargent and Stewart, 1971; Byers and Barnes, 1967]. High-angle faulting was well established prior to the volcanism that began in this area about 16 Ma ago [Marvin *et al.*, 1970]. These relationships suggest that at least some of the extensive faulting in the Tertiary rocks represents reactivation of older structures.

The age of major displacement that is observed on high-angle faults varies within the study area. On Yucca Mountain and in Crater Flat, surface exposures and drill holes provide evidence that most of the displacement on the north trending faults took place between 12.5 and 11.5 Ma ago, that is, between deposition of the Tiva Canyon Member of the Paintbrush Tuff and the Rainier Mesa Member of the Timber Mountain Tuff. The Rainier Mesa Member was deposited across faults bounding structurally elevated blocks of older tuff [Lipman and McKay, 1965]. Much Miocene normal faulting thus took place during a period of voluminous volcanism.

#### Volcano-Tectonic History

Because most of the study area contains thick sequences of tuff and lava and the candidate site area is underlain by more than 2000 m of tuff, a summary of the volcanic history of the study area is warranted.

TABLE 2. Density Measurements of Surface and Drill Hole Samples

Rock Unit	Density, g/cm <sup>3</sup>	
	Unsaturated	Saturated
Older tuff	2.37	...
Older tuff	2.22	...
Older tuff	2.25	...
"Tuff of Lithic Ridge"	2.16	...
Tiva Canyon Member*	2.40	...
Basalt	2.88	...
Rainier Mesa Member†	2.00	2.08
Rainier Mesa Member†	1.86	2.26
Basalt	2.76	...
Basalt cinder	1.39	1.55
Basalt cinder	1.90	2.04
Basalt	2.77	2.78
Basalt	2.88	2.89
Tiva Canyon Member*	2.27	2.30
Tiva Canyon Member*	2.34	2.35
Tuff, undifferentiated	2.84	2.85
Tiva Canyon Member*	2.14	2.36
70 samples of rhyolite of Calico Hills	2.12 ± 0.26	2.26 ± 0.17
Argillite, Eleana Formation	2.59	2.63
Carboniferous argillite	2.59	2.61
Carboniferous argillite	2.58	2.61
Devonian limestone	2.81	2.82
Devonian limestone	2.64	2.67
Devonian dolomite	2.68	2.69
Limestone	2.68	2.70
Limestone,	2.66	2.67
Bonanza King Formation		
Limestone,	2.59	2.62
Bonanza King Formation		
Zabriskie Quartzite	2.64	2.65
Zabriskie Quartzite	2.59	2.60
Zabriskie Quartzite	2.70	2.72
Zabriskie Quartzite	2.61	2.63
Zabriskie Quartzite	2.64	2.64

\*Member of the Paintbrush Tuff.

†Member of the Timber Mountain Tuff.

The stratigraphy of the lower part of the volcanic rock sequence in this area has been studied in detail [Carr *et al.*, 1984], and some revisions in earlier concepts [Byers *et al.*, 1976] have been made. The oldest tuff units at Yucca Mountain, those stratigraphically below the Lithic Ridge Tuff (Table 1), are known from drill holes [Spengler *et al.*, 1981]. The great thickness (more than 600 m) of this older tuff and its position well below sea level suggest accumulation in a sag or collapse feature, possibly a caldera (Figure 2b). The Lithic Ridge Tuff is the oldest extensively exposed volcanic unit in the study area. Its source is unknown, and although penetrated by several drill holes on Yucca Mountain, it is not especially thick in that area. Local occurrences of petrographically similar rhyodacite lava flows above and below the Lithic Ridge Tuff, however, suggest that the source is nearby [Carr *et al.*, 1984].

Next to be deposited in the site area were the three members of the Crater Flat Tuff: in ascending order, the Tram Member, the Bullfrog Member, and the Prow Pass Member. The Crater Flat Tuff has no characteristics in the drill holes at Yucca Mountain which would suggest it was deposited in a caldera there, although the three members have a total thickness of more than 450 m. The source areas or calderas, and greater thicknesses of the Crater Flat Tuff, are thought to lie to the west and northwest of Yucca Mountain, mostly beneath Crater Flat itself (Figure 2) [Carr, 1982; Carr *et al.*, 1984].

The rhyolite lavas and tuff of Calico Hills were emplaced on top of the Crater Flat Tuff in the area between northern Yucca Mountain and the Calico Hills. The main source areas were in the western Calico Hills-Fortymile Canyon area, but some lava reached as far southwest as the northeast edge of Yucca Mountain, where the section consists mostly of about 100 m of bedded air fall and thin ash flow tuff units.

After deposition of the lavas and tuff of the Calico Hills unit, eruptions began from the Timber Mountain-Oasis Valley caldera complex, including the Claim Canyon cauldron segment just north of Yucca Mountain (Figure 2b). These eruptions produced voluminous, widespread ash flow tuff sheets assigned to the Paintbrush Tuff and Timber Mountain Tuff. Regional tumescence or doming is thought to have immediately preceded formation of the complex [Christiansen *et al.*, 1977], and the edge of that uplift may have been near the north end of Yucca Mountain. Very thick sequences of the Paintbrush Tuff and Timber Mountain Tuff accumulated in parts of the caldera complex. During the waning stages of activity at the Timber Mountain center, voluminous lavas and minor tuff were extruded around the edges of the complex. Nearly all the basaltic eruptions followed this stage of activity and have continued into Quaternary time, although volumes have been very small.

#### GRAVITY DATA

More than 2500 gravity measurements have been made in the study area (Figure 1). Each is generally about 2 km from its nearest neighbor. The complete data set analyzed in this report, both new and previously published data, is described by Jansma *et al.* [1982]. Analysis of the complete Bouguer gravity anomalies reduced at the average crustal density of 2.67 g/cm<sup>3</sup> (Figure 4a) was deemed inadequate for the detailed study of the Yucca Mountain area [Snyder and Carr, 1982]. Density measurements discussed previously indicate that rocks making up much of the topographic relief in volcanic terrane of this area have densities between 1.7 and 2.3 g/cm<sup>3</sup>, averaging 2.0 g/cm<sup>3</sup>. The complete Bouguer anomalies were,

therefore, reduced a second time, according to the method of R. W. Saltus (written communication, 1980), at a density of 2.0 g/cm<sup>3</sup>. Thus gravity effects attributable to the topographic distribution of the stations within volcanic terrane have been eliminated.

To remove some of the effects attributable to lateral density variations deeper than 5 km within the crust, an isostatic correction was also applied to the complete Bouguer anomalies (Figure 4b). This correction assumes that complete Airy-Heiskanen isostatic compensation occurs at the Moho throughout the earth; although Airy-type isostasy may not strictly apply to southern Nevada, the gravitational effect of any compensating mass is indistinguishable from Airy compensation at the scale of this study [Jachens and Griscom, 1983]. The calculations were made by using the computer procedure of Jachens and Roberts [1981] and assuming a mean crustal thickness at sea level of 25 km, a surface topography density of 2.67 g/cm<sup>3</sup>, and a density contrast of 0.4 g/cm<sup>3</sup> across the Moho within a 167-km distance from Yucca Mountain [Jachens and Griscom, 1983]. Preliminary work (H. W. Oliver, written communication, 1983) adjusting the parameters in the isostatic correction computations indicates that in central Nevada a more appropriate reference mean crustal thickness at sea level may be 16-18 km; calculated crustal thicknesses between 25 and 35 km result for those parts of Nevada where average elevation is 1-2 km. However, in the present study, the purpose of this isostatic correction was not to estimate the deep crustal structure beneath Yucca Mountain, but to filter out long-wavelength gravity effects related to the compensation of surface topography.

The final product of all these corrections and reductions is a model with rocks of 2.0-g/cm<sup>3</sup> density above the lowest gravity station elevation in the study area, rocks of 0.4-g/cm<sup>3</sup> density contrast across the Moho within its vertical range at depths of about 30 to 40 km locally [Johnson, 1965], and rocks of homogeneous lateral densities elsewhere. Further modeling begins with this simple and basic model and, drawing on geologic and geophysical evidence, attempts to further characterize the rocks near the earth's surface by comparing the gravity field in the models with that actually observed.

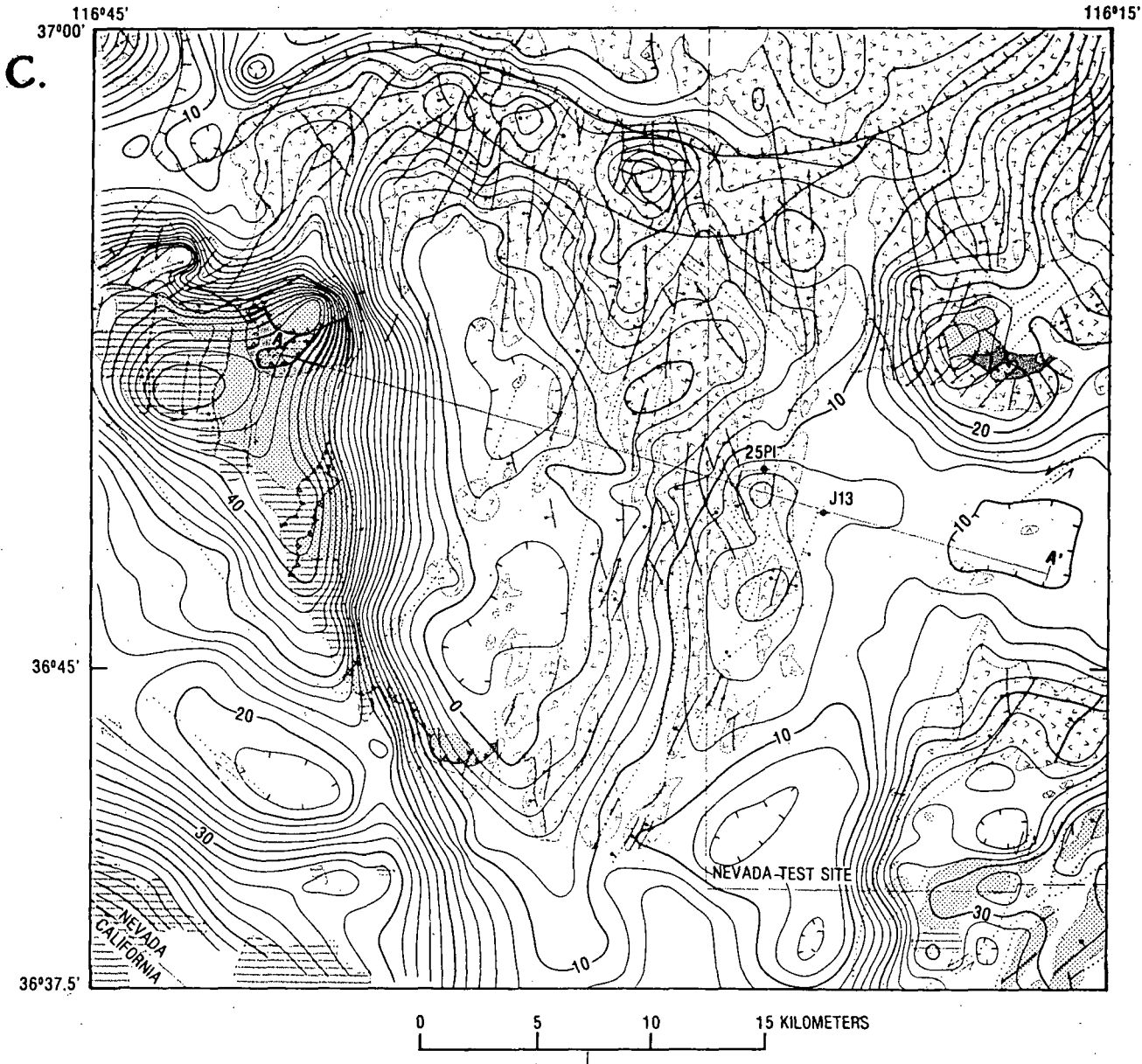
#### INTERPRETATION OF THE GRAVITY FIELD

Three analytical tools aided the interpretation of the gravity field at Yucca Mountain: a 2-mGal contour map (Figure 4c; Snyder and Carr [1982]) reduced at 2.00 g/cm<sup>3</sup> and corrected for perfect isostasy, a two-dimensional modeled cross section extending east-west across the study area (Figures 4c and 5), and a three-dimensional multiple-polygon gravity model (Figures 5 and 6). The three-dimensional model [Plouff, 1975], using simple flat polygonal source bodies, provided more accurate depth estimates; it consisted of eight bodies of prevolcanic rocks, three bodies of the dense tuff of Chocolate Mountain, two bodies composed of the Crater Flat Tuff, and one alluvial body along Topopah Wash. This simple model approximates the observed gravity field to within 3 mGal in the area near Yucca Mountain and Crater Flat.



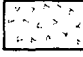
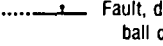



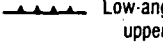
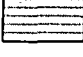
#### Bare Mountain Gravity High

The most distinctive gravity feature within the study area is the approximately rectangular anomaly along the western border of the area, which generally coincides with Bare Mountain and the Funeral Mountains, interrupted by the northwest trending Amargosa Valley (Figures 1 and 4c). Residual gravity values greater than 14 mGal delimit the anomaly. The rocks





EXPLANATION

- |   |   |   |  |
|---|---|---|--|
|  | Alluvium (Quaternary and Tertiary)                                    |  | Contact  |
|  | Volcanic rocks (Quaternary and Tertiary)                              |  | Fault, dotted where concealed; bar and ball on downthrown side |
|  | Sedimentary rocks (upper Paleozoic)—Mainly clastic rocks              |  | Caldera wall   |
|  | Sedimentary rocks (middle and lower Paleozoic)—Mainly carbonate rocks |  | Low-angle fault or glide plane; teeth on upper plate           |
|  | Sedimentary rocks (lower Paleozoic and Precambrian)—Clastic rocks     |   |  |


 Gravity contours; contour interval is 2 mGal; hachures indicate areas of low gravity values.

Fig. 4c. Isostatic residual gravity and geologic map of the Yucca Mountain-Crater Flat area (Figure 1). Gravity values are isostatically corrected and reduced at 2.0 g/cm<sup>3</sup>. A-A' is profile of Figure 5.

19.8  
27.2

188

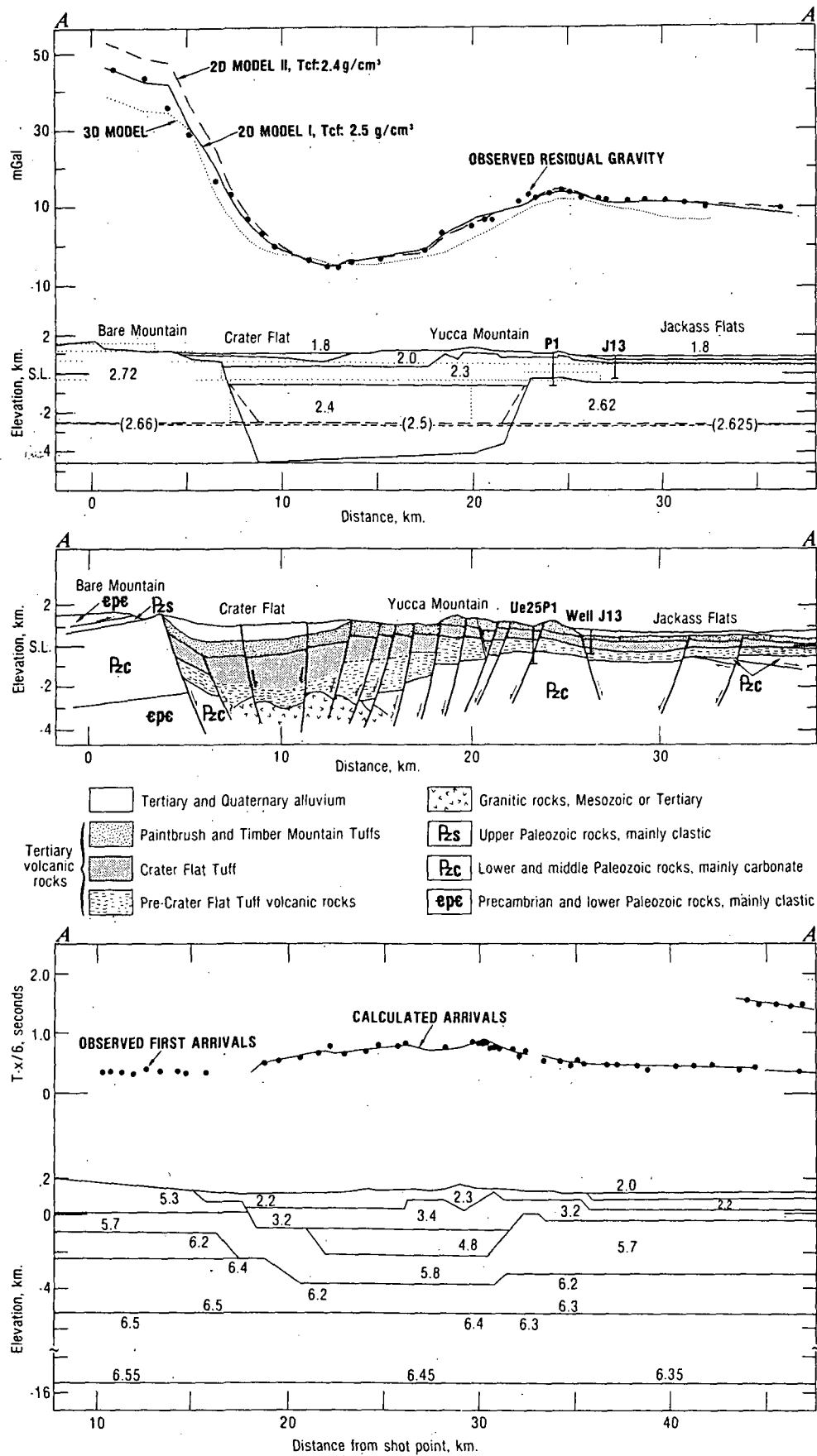


Fig. 5. Gravity, geologic, and seismic refraction cross sections along profile A-A' (Figure 4). Numbers represent bulk densities (grams per cubic centimeters) and velocities (kilometers per second) of the modeled bodies in the gravity and seismic cross sections, respectively. The three-dimensional model densities are the same as those of two-dimensional model II. Two two-dimensional gravity models are indicated: the density and thickness of the buried Crater Flat Tuff were varied; densities in parentheses were used in model I. The thrust shown near A' on the geologic cross section is an interpretation based upon the regional distribution of the Eleana Formation and the thick middle and lower Paleozoic carbonate rocks. Seismic section modified from Hoffman and Mooney [1983].

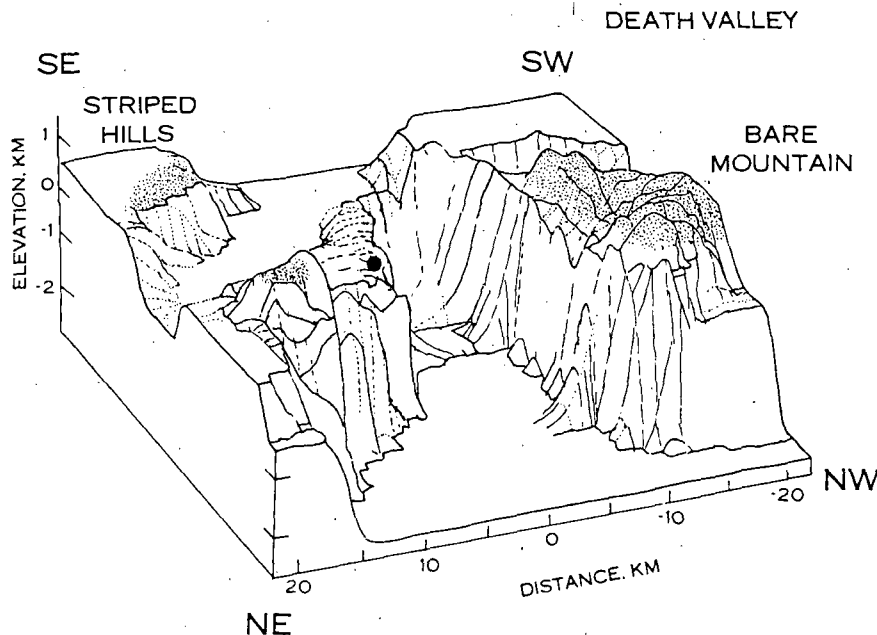


Fig. 6. Mesh perspective of prevolcanic rock unit bodies in the three-dimensional gravity model. The mesh surface represents the pretuff surface beneath the topographic surface. Stippling shows where these surfaces coincide at Bare Mountain, at the Striped Hills, and at the Calico Hills (in left center). Flat surface at elevation of  $-2.5$  km is due to lack of resolution of the gravity method at this depth and greater depths. Repository site on the east side of Yucca Mountain lies about 1 km above shaded circle.

of Bare Mountain and the Funeral Range are Precambrian and Paleozoic limestone, dolomite, argillite, and quartzite; some are locally recrystallized. These rocks have some of the highest densities in the study area. As a result, the observed anomaly (Figures 4 and 5) is accentuated an additional 10 mGal by the reduction density of  $2.00 \text{ g/cm}^3$  because the rock densities of measured surface samples actually range from  $2.59$  to  $2.70 \text{ g/cm}^3$ .

The gravity feature indicates a continuous block of Precambrian and Paleozoic rocks stretching from the eastern edge of Death Valley, across the Amargosa Valley, to the northern edge of Bare Mountain. The gravity saddle coincident with the Amargosa River is not deep enough to result from an absence of dense rock at depth but probably results from a thick accumulation of Tertiary volcanic and sedimentary rocks underlying the alluvium of Amargosa Valley, possibly augmented by dip-slip faults and extensional grabens related to the Walker Lane. These faults may have created structural downwarps or basins that collected sufficient alluvium from Bare Mountain to account for the lower gravity values. The detailed shape of the gravity curve over the east flank of Bare Mountain in profile (Figure 5) suggests that the Paleozoic rocks extend several kilometers farther eastward beneath Crater Flat than the surface contacts indicate.

The unusually high gravity values at the Funeral Mountains and Bare Mountain complicate the use of Bare Mountain as a reference area against which to compare the gravity over the rest of the study area. After adjustment is made for the surface geology in the three-dimensional modeling, the calculated gravity values at Bare Mountain still are not great enough to match the observed values; this disagreement indicates an underlying mass excess relative to the gravity model. The bulk density of about  $2.72 \text{ g/cm}^3$  used in the model may be somewhat low; the Funeral Mountains consist largely of Precambrian rocks, most of which are metamorphosed, and

Bare Mountain may contain a low-angle fault underlain by more strongly metamorphosed rocks [Monsen, 1983]. Preliminary seismic refraction results (Hoffman and Mooney [1983]; Figure 5) confirm density-velocity heterogeneity within the Bare Mountain block. Rock densities as high as  $2.8$  or  $2.9 \text{ g/cm}^3$  are possible based on the seismic velocities modeled within Bare Mountain and velocity-density relationships in southern Nevada [Hill, 1978, Figure 7-11].

#### Calico Hills Gravity High

If defined by the local 22-mGal contour (Figure 4c), the Calico Hills gravity anomaly may be interpreted to support the structural dome hypothesis of Maldonado et al. [1979]. If expanded to include the 14-mGal contour, the anomaly is no longer closed and extends farther to the northeast. Further, the gravity high enclosed by the 14-mGal contour to the southwest of the Calico Hills near Busted Butte (Figure 1) appears to extend this trend of gravity highs in that direction. Data from the UE25P-1 drill hole further support this observation, as pre-Tertiary rocks similar to those exposed at the Calico Hills were penetrated at depths of about 1250 m. Buried high topography on Paleozoic rocks along the eastern borders of the Timber Mountain and Crater Flat-Prospector Pass caldera complexes could explain the local gravity highs along this trend. The lesser thickness of volcanic rocks in the Busted Butte-Calico Hills area, as suggested by the gravity modeling, may have resulted in the faulting of a different trend and intensity than that observed in the central part of Yucca Mountain, where the volcanic rocks are over twice as thick.

The 10-mGal gravity saddle between the Calico Hills high and the Busted Butte high (Figure 4c) is on the trend of Yucca Wash (Figure 1), a conspicuous northwest trending valley bounding northeastern Yucca Mountain. A fault zone, pre-Paintbrush Tuff in age, is suspected along Yucca Wash on the

basis of rock unit distributions; this structure may interrupt or offset the buried prevolcanic surface discussed above.

#### Crater Flat–Yucca Mountain Gravity Low

A large, roughly triangular gravity low, defined by the 8-mGal residual gravity contour, dominates the gravity field in the study area (Figure 4c). The most striking feature of this anomaly is that it includes not only the topographically low area of Crater Flat but also some of the high ramparts of Yucca Mountain. The anomaly extends northeastward from Bare Mountain nearly to the Calico Hills.

The three-dimensional model indicates that the volcanic rocks extend to at least 2500 m below sea level beneath Crater Flat (Figure 6). These relatively low density rocks, which lie about 10 km south of the Timber Mountain caldera [Byers *et al.*, 1976], may be material filling a combination of sector grabens and old calderas, probably the source areas for the Crater Flat Tuff. This gravity low extends 50 km to the south of the study area, along the Amargosa Desert Valley, and into the northern Greenwater Range, which contains a 4- to 8-Ma-old volcanic field. Although the graben structures may extend southward beyond the south edge of the study area, the caldera features do not.

Estimates of the tuff thickness beneath Crater Flat are minima. Tuff density below 2000-m depths, as indicated by the log measurements in the deep drill holes at Yucca Mountain, is greater than 2.5 g/cm<sup>3</sup>, probably greater than 2.6 g/cm<sup>3</sup> if the linear increase in density continues beneath the drilled depths (Figure 3). Neighboring caldera wallrocks are thought to be mostly Paleozoic sedimentary rocks; metamorphism or hydrothermal alteration may have either increased or decreased the bulk density of these rocks. Surface sample measurements on the Paleozoic rocks indicate densities between 2.6 and 2.7 g/cm<sup>3</sup>; densities may be slightly increased by 3 km of overburden. As a result of these uncertainties, the density contrast between intracaldera rocks and the caldera wallrocks may range from -0.2 to +0.1 g/cm<sup>3</sup> at 4.0 km below sea level, the estimated floor of the caldera fill. Floor elevation uncertainties of ±2.0 km or greater (Figure 5) are possible from this range of density contrast. The seismic refraction model achieved the best match between observed and calculated delay times by assuming the caldera floor rocks (5.8-km/s body in Figure 5) to lie between 2 and 4 km below sea level.

The -2-mGal closures in the northern and southern parts of the Crater Flat anomaly are separated by a narrow band of higher gravity values anchored by protruding positive anomalies. This configuration of the gravity field suggests a septum or ridge of higher density rocks cutting across the depression at this point. Relations in the Crater Flat Tuff and associated volcanic rocks suggest that Crater Flat may contain the source areas for this tuff and related lavas [Carr, 1982]. The septum suggested by the slight gravity deflections may separate two source and collapse areas. The 0-mGal closure to the northeast of the Crater Flat gravity low correlates with a postulated "older tuff" caldera or sag feature (Figure 2).

#### Chocolate Mountain Gravity High

A narrow band of gravity highs (Figure 4c), peaking at 14, 12, and 16 mGal, separates the large negative anomalies associated with Crater Flat and those associated with the Timber Mountain caldera to the north. The most prominent gravity high along this band coincides with Chocolate Mountain (Figure 1) and the Claim Canyon cauldron segment

(Figure 2; Byers *et al.* [1976]). The three-dimensional model indicates that more than 4000 m of material with density contrasts between +0.2 and 0.3 g/cm<sup>3</sup> would be necessary to cause the observed anomalies.

The Claim Canyon cauldron segment is an eccentric resurgent block of the very thick, densely welded intracaldera Tiva Canyon Member and other related parts of the Paintbrush Tuff [Byers *et al.*, 1976]. Samples collected at Chocolate Mountain yielded an average density of 2.32 ± 0.12 g/cm<sup>3</sup>. The absence of a depression or moat, filled with relatively low density rock, that is commonly associated with a caldera emphasizes this gravity high. The western part of this relatively narrow gravity high, in the northwestern part of Yucca Mountain, appears to be due largely to a combination of the thick dense intracaldera Paintbrush Tuff, as at Chocolate Mountain, and of the thick, densely welded Tram Member of the Crater Flat Tuff exposed outside the Timber Mountain–Oasis Valley caldera complex. The tram Member exposed in this area may also be part of a fragmented resurgent dome (Figure 2).

North of Chocolate Mountain is the edge of a gravity low directly associated with the Timber Mountain caldera [Kane and Webring, 1981]. This gravity low, which is related to the Timber Mountain and Silent Canyon calderas, is the most conspicuous one in southern Nevada (Figure 4a).

#### DISCUSSION

The present gravity study clearly defines the proposed waste repository site as lying adjacent to one of the most voluminous Tertiary caldera complexes in the western United States. The central gravity low on the residual gravity map (Figure 4c) represents a large tuff-filled hole or depression in the Tertiary rocks beneath both Crater Flat and parts of Yucca Mountain (Figure 6). A minimum thickness of 1830 m of tuff beneath Yucca Mountain is confirmed by drill holes. Reference gravity values above known Paleozoic rocks at drill hole UE25P-1, and at outcrops in the Calico Hills and the Striped Hills, give a modeling estimate of at least 4000 m of tuffaceous fill in the Crater Flat–Yucca Mountain depression.

In addition to the gravity evidence, surface geologic relations and information from drill holes strongly suggest that Crater Flat is the source area for all three members of the Crater Flat Tuff. The gravity saddle separating the northern and southern minima in Crater Flat may indicate two structures: a caldera associated with the Tram Member in the northern part of Crater Flat and a caldera associated with the Bullfrog Member and Prow Pass Member in the southern part of Crater Flat. These two collapse areas may be separated by a narrow septum of Paleozoic rocks, or possibly lava flows, beneath central Crater Flat. It is unlikely, however, that the lobe of the gravity low extending northeastward beneath Yucca Mountain is part of the collapse area related to the Crater Flat Tuff. The Crater Flat Tuff is nearly as thick in well J-13 as it is in drill hole G1 within the gravity low lobe. Therefore the northeastern lobe of the gravity low at Yucca Mountain is unrelated to the Crater Flat Tuff and is related to either a structural depression, possibly a caldera, within which thick units older than the Crater Flat Tuff accumulated or altered upper Paleozoic rocks with densities of 2.5–2.6 g/cm<sup>3</sup> underlying the tuff in this location.

The recognition of the Crater Flat–Prospector Pass calderas adds nearly 350 km<sup>2</sup> to the total 1500-km<sup>2</sup> area of caldera collapse associated with the southwestern Nevada volcanic field. Considered together, the Timber Mountain caldera

complex and its satellite calderas form one of the largest caldera systems in the western United States. Only the Long Valley caldera [Kane *et al.*, 1976] and the Yellowstone caldera [Eaton *et al.*, 1975; Lehman *et al.*, 1982] compare in areal extent, 550 and 3300 km<sup>2</sup> versus 1800 km<sup>2</sup>, and in magnitude of the associated negative gravity anomaly, 50 and 60 mGal versus 60 mGal, with the Timber Mountain complex.

The gravity high that extends southwestward from the northeast corner of the study area is interpreted to reflect a shallowly buried, Paleozoic rock surface. Indeed, Paleozoic rocks crop out at several places along this high, for example, in the Calico Hills and the Eleana Range (Figure 1). The Eleana Range, the Calico Hills, and the Paleozoic rocks beneath Busted Butte may all be part of a topographically high pre-Miocene surface, underlain predominantly by argillite of the Eleana Formation, that was partly covered by Tertiary tuff. This ridge of Paleozoic rocks could also be viewed as an eroded escarpment facing the Crater Flat-Timber Mountain-Silent Canyon caldera complexes. We suggest that the down-to-the-east faults, unusual near Yucca Mountain, in the area of Busted Butte [Lipman and McKay, 1965] are the result of drag and shear of the tuff near the intersection of northwest and northeast trending shear zones (Figure 2). The expression of this structure may be enhanced by the thinner tuff cover in this area.

An important question is the possible existence of a large east-west trending intrusive body beneath the area. Evidence for such a body includes a distinct east-west trending lineament of several parallel contours on the 2440-m constant-barometric-elevation aeromagnetic map of the area [Boynton and Vargo, 1963] that coincides roughly with the southeast border of the northeastern lobe of the central gravity low. Very little difference in the upper part of the tuff section occurs across this lineament, as shown by the similarity of the units encountered in drill holes north and south of it, but significant magnetic property changes may occur in the middle part of the section which includes a Bullfrog Member variable in thickness and local dacitic lava flows. The distribution of these changes in units, however, does not appear to correspond closely with the aeromagnetic lineament. The gravity modeling is ambiguous with regard to a deep intrusive body. All the gravity anomalies can be adequately accommodated by density contrasts at the Paleozoic-Tertiary unconformity, assuming that all the pre-Tertiary rocks are non-igneous. Part of the gravity low in the center of the study area could also be produced by a large shallow intrusive mass, a possibility favored by the relative paucity of major faults in this vicinity if a large intrusive body acted as a structurally stabilizing mass for overlying units at Yucca Mountain.

The depth and extent of an intrusive body beneath the nearby Calico Hills remain unresolved [Snyder and Oliver, 1981]. Extensive hydrothermal and contact-metamorphic alteration of the rocks in drill hole UE25a-3 [Maldonado *et al.*, 1979], the high heat flow of 3.2 HFU [Sass *et al.*, 1980], and topographic uplift (D. L. Hoover, written communication, 1982) all suggest, but of course do not prove, the existence of an intrusive body beneath the Calico Hills. At Bare Mountain, metamorphism [Monsen, 1983] and a granitic dike of probable Mesozoic age similarly suggest the presence of plutonic rock at depth.

Estimates based on the aeromagnetic contours between the Calico Hills and Yucca Mountain [Boynton and Vargo, 1963] indicate that the source of the anomaly, possibly a granitic pluton with a magnetite replacement halo, is 2200 m or more

deep (G. D. Bath, unpublished data, 1981). These depths are near the bottom of the gravity models and would require differentiation between carbonate rocks, argillite, and intrusive rocks beneath a thick tuff overburden. At that depth, these rocks have similar densities and would be difficult to distinguish without precise thickness estimates and density control of the overlying rocks; this gravity study cannot independently determine whether the tuff grades downward into a crystallized magma body or rests atop a downdropped block of pre-Tertiary rocks.

Both seismic refraction studies (Figure 5; Mooney *et al.* [1982]) and teleseismic experiments [Monfort and Evans, 1982] have shown that high-velocity rocks underlie the Yucca Mountain region. Velocities as high as 6.55 km/s are tentatively inferred to lie at depths as shallow as 15 km. The high velocities here may be caused by either mafic sills, dikes, or diapirs that were involved in the extensive Miocene volcanism of the area and the more recent basaltic eruptions in Crater Flat or by metamorphosed sedimentary and crystalline rocks such as those exposed at Bare Mountain and in the Funeral Mountains. The mafic intrusives may be related to the riftlike graben structure of Crater Flat and be part of an extensional zone accommodating right-lateral movement within the Walker Lane [Wernicke *et al.*, 1982]; the regional metamorphism may have resulted from heat associated with the eruptions of the Timber Mountain caldera complex [Monsen, 1983]. Without density measurements from depths greater than 2-3 km, gravity modeling cannot independently resolve rock configurations at the base of the intracaldera fill. Simultaneous inversion of velocity and density data to match gravity and seismic observations could better resolve structural-tectonic questions related to the subsidence history of the calderas, questions concerning the existence of mafic intrusive or metamorphosed wall rock within the collapsed area, and the possibility that low-angle faults separate brittle rock cut by numerous high-angle faults from plastically deformed metamorphosed basement rock beneath Crater Flat, Bare Mountain, and to the west toward Death Valley.

*Acknowledgments.* H. W. Oliver is due many thanks for his encouragement, advice, and guidance throughout this gravity study. We are also grateful to the many scientists investigating the suitability of Yucca Mountain as a waste isolation site for freely sharing their data and thoughts, in particular: G. D. Bath, F. M. Byers, Jr., M. D. Carr, D. L. Healey, D. B. Hoover, W. D. Mooney, D. A. Ponce, G. D. Robinson, and R. W. Spengler. Diligent field work by several members of the U.S. Geological Survey and Fenix and Sisson, Inc., was much appreciated. This research was in part supported by the Nevada Operations Office of the U.S. Department of Energy.

#### REFERENCES

- Albers, J. P., Belt of sigmoidal bending and right lateral faulting in the western Great Basin, *Geol. Soc. Am. Bull.* 78, 143-156, 1967.
- Boynton, G. R., and J. L. Vargo, Aeromagnetic map of the Topopah Spring quadrangle and part of the Bare Mountain quadrangle, Nye County, Nevada, *Geophys. Inv. Map GP-440*, U.S. Geol. Surv., Washington, D. C., 1963.
- Byers, F. M., Jr., and H. Barnes, Geologic map of the Paiute Ridge quadrangle, Nye and Lincoln counties, Nevada, *Geol. Quad. Map GQ-577*, U.S. Geol. Surv., Washington, D. C., 1967.
- Byers, F. M., Jr., W. J. Carr, P. P. Orkild, W. D. Quinlivan, and K. A. Sargent, Volcanic suites and related cauldrons of Timber Mountain-Oasis Valley caldera complex, southern Nevada, *U.S. Geol. Surv. Prof. Pap.* 919, 70 pp., 1976.
- Carr, W. J., Summary of tectonic and structural evidence for stress orientation at the Nevada Test Site, *U.S. Geol. Surv. Open File Rep.* 74-176, 53 pp., 1974.
- Carr, W. J., Volcano-tectonic history of Crater Flat, southwestern Nevada, as suggested by new evidence from drill hole USW-VH-1

- and vicinity, *U.S. Geol. Surv. Open File Rep.*, 82-457, 23 pp., 1982.
- Carr, W. J., and W. D. Quinlivan, Structure of Timber Mountain resurgent dome, Nevada Test Site, *Mem. Geol. Soc. Am.*, 110, 99-108, 1968.
- Carr, W. J., and A. M. Rogers, Tectonics, seismicity and erosion rates in the southern Great Basin, *U.S. Geol. Surv. Open File Rep.*, 82-509, 11-15, 1982.
- Carr, W. J., F. M. Byers, Jr., and P. P. Orkild, Stratigraphic and volcano-tectonic relations of Crater Flat Tuff, and some older volcanic units, Nye County, Nevada, *U.S. Geol. Surv. Prof. Pap.*, 1323, in press, 1984.
- Christiansen, R. L., P. W. Lipman, W. J. Carr, F. M. Byers, Jr., P. P. Orkild, and K. A. Sargent, Timber Mountain-Oasis Valley caldera complex of southern Nevada, *Geol. Soc. Am. Bull.*, 88, 943-959, 1977.
- Cornwall, H. R., and F. J. Kleinhampl, Geology of the Bare Mountain quadrangle, Nevada, *Geol. Quad. Map GQ-157*, U.S. Geol. Surv., Washington, D. C., 1961.
- Crowe, B. M., D. T. Vaniman, and W. J. Carr, Status of volcanic hazard studies for the Nevada nuclear waste storage investigations, *Rep. LA-9325-MS*, Los Alamos Natl. Lab., Los Alamos, N. M., 1983.
- Eaton, G. P., R. L. Christiansen, H. M. Iyer, A. M. Pitt, D. R. Mabey, H. R. Blank, Jr., I. Zietz, and M. E. Gettings, Magma beneath Yellowstone National Park, *Science*, 188, 787-796, 1975.
- Ekren, E. B., and K. A. Sargent, Geologic map of the Skull Mountain quadrangle, Nye County, Nevada, *Geol. Quad. Map GQ-387*, U.S. Geol. Surv., Washington, D. C., 1965.
- Healey, D. L., and C. H. Miller, Gravity survey of the Amargosa Desert of Nevada and California, *Rep. USGS-474-136*, 30 pp., U.S. Geol. Surv., Washington, D. C., 1971.
- Hill, D. P., Seismic evidence for the structure and Cenozoic tectonics of the Pacific coast states, *Mem. Geol. Soc. Am.*, 152, 145-147, 1978.
- Hoffman, L. R., and W. D. Mooney, A seismic study of Yucca Mountain and vicinity, southern Nevada: Data report and preliminary results, *U.S. Geol. Surv. Open File Rep.*, 83-588, 57 pp., 1983.
- Jachens, R. C., and A. Griscom, Three-dimensional geometry of the Gorda Plate beneath northern California, *J. Geophys. Res.*, 88, 9375-9392, 1983.
- Jachens, R. C., and C. W. Roberts, Documentation of a FORTRAN program, "isocomp," for computing isostatic residual gravity, *U.S. Geol. Surv. Open File Rep.*, 81-574, 26 pp., 1981.
- Jansma, P. E., D. B. Snyder, and D. A. Ponce, Principal facts of gravity stations with gravity and magnetic profiles from the southwest Nevada Test Site, Nye County, Nevada, as of January, 1982, *U.S. Geol. Surv. Open File Rep.*, 82-1041, 43 pp., 1982.
- Johnson, L. F., Crustal structure between Lake Mead, Nevada, and Mono Lake, California, *J. Geophys. Res.*, 70, 2863-2872, 1965.
- Kane, M. F., and M. W. Webring, A preliminary analysis of gravity and aeromagnetic surveys of the Timber Mountain area, southern Nevada, *U.S. Geol. Surv. Open File Rep.*, 81-189, 43 pp., 1981.
- Kane, M. F., D. R. Mabey, and R.-L. Brace, A gravity and magnetic investigation of the Long Valley caldera, Mono County, California, *J. Geophys. Res.*, 81, 754-762, 1976.
- Lehman, J. A., R. B. Smith, and M. M. Schilly, Upper crustal structure of the Yellowstone caldera from seismic delay time analyses and gravity correlations, *J. Geophys. Res.*, 87, 2713-2730, 1982.
- Lipman, P. W., and E. J. McKay, Geologic map of the Topopah Spring SW quadrangle, Nye County, Nevada, *Geol. Quad. Map GQ-439*, U.S. Geol. Surv., Washington, D. C., 1965.
- Locke, A., P. R. Billingsley, and E. B. Mayo, Sierra Nevada tectonic pattern, *Geol. Soc. Am. Bull.*, 51, 513-540, 1940.
- Maldonado, F., and S. L. Koether, Stratigraphy, structure, and some petrographic features of Tertiary volcanic rocks at the USW-G2 drill hole, Yucca Mountain, Nye County, Nevada, *U.S. Geol. Surv. Open File Rep.*, 83-732, 83 pp., 1983.
- Maldonado, F., D. C. Muller, and J. N. Morrison, Preliminary geologic and geophysical data of the UE25a-3 exploratory drill hole, Nevada Test Site, Nevada, *Rep. USGS-1543-6*, 43 pp., U.S. Geol. Surv., Washington, D. C., 1979.
- Marvin, R. F., F. M. Byers, Jr., H. H. Mehnert, P. P. Orkild, and T. W. Stern, Radiometric ages and stratigraphic sequence of volcanic and plutonic rocks, southern Nye and western Lincoln counties, Nevada, *Geol. Soc. Am. Bull.*, 81, 2657-2676, 1970.
- Monfort, M. E., and J. R. Evans, Teleseismic studies of the earth's crust and upper mantle in southern Nevada (abstract), *Eos Trans. AGU*, 63, 1099, 1982.
- Monsen, S. A., Structural evolution and metamorphic petrology of the Precambrian strata, northwest Bare Mountain, Nevada, M.S. thesis, Univ. of Calif., Davis, 1983.
- Mooney, W. D., D. B. Snyder, and L. R. Hoffman, Seismic refraction and gravity modeling of Yucca Mountain, Nevada Test Site, southern Nevada (abstract), *Eos Trans. AGU*, 63, 1100, 1982.
- Plouff, D., Derivation of formulas and FORTRAN programs to compute gravity anomalies of prisms, *Rep. USGS-GD-75-915*, 90 pp., U.S. Geol. Surv., Washington, D. C., 1975.
- Ponce, D. A., Preliminary gravity investigations of the Wahmonie Site, Nevada Test Site, Nye County, Nevada, *U.S. Geol. Surv. Open File Rep.*, 81-522, 64 pp., 1981.
- Poole, F. G., Flysch deposits of the Antler foreland basin, western United States, in *Tectonics and Sedimentation*, *Spec. Publ. 22*, edited by W. R. Dickinson, pp. 58-82, Society of Economic Paleontologists and Mineralogists, Tulsa, Okla., 1974.
- Robbins, S. L., J. W. Schmoker, and T. C. Hester, Principal facts and density estimates for borehole gravity stations in exploratory wells Ue5ah, Ue7, Ue1h, Ue1q, Ue2co, and USW-H1 at the Nevada Test Site, Nye County, Nevada, *U.S. Geol. Surv. Open File Rep.*, 82-277, 33 pp., 1982.
- Sargent, K. A., and J. H. Stewart, Geologic map of the Specter Ranger N. W. quadrangle, Nye County, Nevada, *Geol. Quad. Map GQ-384*, U.S. Geol. Surv., Washington, D. C., 1971.
- Sass, J. H., A. H. Lachenbruch, and C. W. Mase, Analysis of thermal data from drill holes UE25a-3 and UE25a-1, Calico Hills and Yucca Mountain, Nevada Test Site, *U.S. Geol. Surv. Open File Rep.*, 80-826, 25 pp., 1980.
- Snyder, D. B., and W. J. Carr, Preliminary results of gravity investigations at Yucca Mountain and vicinity, southern Nye County, Nevada, *U.S. Geol. Surv. Open File Rep.*, 82-701, 36 pp., 1982.
- Snyder, D. B., and H. W. Oliver, Preliminary results of gravity investigations of the Calico Hills, Nevada Test Site, Nye County, Nevada, *U.S. Geol. Surv. Open File Rep.*, 81-101, 42 pp., 1981.
- Spengler, R. W., F. M. Byers, Jr., and J. B. Warner, Stratigraphy and structure of volcanic rocks in drill hole USW-G1, Yucca Mountain, Nye County, Nevada, *U.S. Geol. Surv. Open File Rep.*, 81-1349, 50 pp., 1981.
- Stewart, J. H., Geology of Nevada, *Spec. Publ. 4*, 136 pp., Nev. Bur. of Mines and Geol., Carson City, 1980.
- U.S. Geological Survey, Aeromagnetic map of parts of the Goldfield, Mariposa, and Death Valley 1° by 2° quadrangles, Nevada-California, *Geophys. Inv. Map GP-753*, Washington, D. C., 1971.
- U.S. Geological Survey, Aeromagnetic map of Lathrop Wells area, Nevada, *Open File Map 78-1103*, Washington, D. C., 1978.
- U.S. Geological Survey, Aeromagnetic map of the Timber Mountain area, Nye County, Nevada, *Open File Map 79-587*, Washington, D. C., 1979.
- Vaniman, D., B. M. Crowe, E. Gladney, W. J. Carr, and R. J. Fleck, Geology and petrology of the Crater Flat and related volcanic fields, south-central Great Basin, Nevada (abstract), *Geol. Soc. Am. Abstr. Programs*, 12, 540, 1980.
- Waters, A. C., and P. R. Carroll (Eds.), Preliminary stratigraphic and petrologic characterization of core samples from USW-G1, Yucca Mountain, Nevada, *Rep. LA-8840-MS*, 66 pp., Los Alamos Natl. Lab., Los Alamos, N. Mex., 1981.
- Wernicke, B., J. E. Spencer, B. C. Burchfiel, and P. L. Guth, Magnitude of extension in the southern Great Basin, *Geology*, 10, 499-502, 1982.

W. J. Carr, U.S. Geological Survey, Box 25046, Denver Federal Center, Denver, CO 80225.

D. B. Snyder, Department of Geological Sciences, Cornell University, Ithaca, NY 14853.

(Received November 14, 1983;  
revised March 12, 1984;  
accepted May 25, 1984.)

## Role of Geophysics in Identifying and Characterizing Sites for High-Level Nuclear Waste Repositories

JEFFREY C. WYNN AND EUGENE H. ROSEBOOM

U.S. Geological Survey, Reston, Virginia

Evaluation of potential high-level nuclear waste repository sites is an area where geophysical capabilities and limitations may significantly impact a major governmental program. Since there is concern that extensive exploratory drilling might degrade most potential disposal sites, geophysical methods become crucial as the only nondestructive means to examine large volumes of rock in three dimensions. Characterization of potential sites requires geophysicists to alter their usual mode of thinking: no longer are anomalies being sought, as in mineral exploration, but rather their absence. Thus the size of features that might go undetected by a particular method take on new significance. Legal and regulatory considerations that stem from this different outlook, most notably the requirements of quality assurance (necessary for any data used in support of a repository license application), are forcing changes in the manner in which geophysicists collect and document their data.

### INTRODUCTION

The search for disposal sites for high-level radioactive wastes from commercial nuclear reactors continues worldwide with increasing intensity and resources. While possible seabed disposal is being carefully studied, by far the largest efforts have gone into seeking possible repositories in deep, stable geologic formations on land. In the United States the Department of Energy (DOE) has responsibility for solving the waste disposal problem for high-level nuclear wastes produced by commercial reactors. The U.S. Geological Survey advises and assists DOE and its contractors in the earth science aspects of this task and conducts research on techniques of exploration and characterization as well as on natural processes related to disposal [Schneider and Trask, 1982]. The Batelle Institute, Rockwell International, Woodward-Clyde Consultants, and Law Engineering are some of the private organizations that work on major subtasks of the larger problem, along with several of the national laboratories such as Sandia, Los Alamos, and Lawrence Berkeley laboratories.

The Nuclear Waste Policy Act of 1982 (NWPA) has legislated the general sequence of activities, defined the political and regulatory process, and set a schedule for the construction of the first two mined nuclear waste repositories to be established in the United States. For each repository, at least five candidate sites are to be nominated initially. From among these, three are to be further evaluated by exploratory shafts and detailed site characterization.

The information obtained from the initial exploration phase and subsequent detailed studies and tests will be the technical basis on which a final selection is made. This information will also be required to justify a subsequent license application to the Nuclear Regulatory Commission (NRC). For any repository site selected, DOE will have to demonstrate that the limits for future possible concentrations of nuclides set by the Environmental Protection Agency (currently in draft form) will not be exceeded and that the technical criteria established by NRC for licensing a repository are satisfied.

Nine candidate sites (Figure 1) were identified by DOE for the first proposed repository; according to the NWPA schedule, three of these sites were selected by the President in De-

cember 1984 for detailed site characterization and construction of exploratory shafts by 1985. Final construction at one site should begin by 1991. Two candidate sites were identified in volcanic rocks on DOE reservations (one in basalts at the Hanford site, Washington, and one in ash flow tuffs at the Nevada Test Site), four were in bedded salt (two in the Paradox Basin, Utah, and two in the Palo Duro Basin, Texas), and three were in salt domes (two in Mississippi and one in Louisiana) [Smedes, 1982; U.S. Department of Energy, 1982, 1984a, b, c, d, e]. In December 1984, DOE announced that the Hanford Reservation in southeastern Washington State, Yucca Mountain at the Nevada Test Site in southern Nevada, and Deaf Smith County in the Permian Basin of Texas have been proposed for the detailed site characterization.

An additional site is being studied by the DOE for military wastes; this is the Waste Isolation Pilot Project (WIPP) located in southeastern New Mexico. This site is being independently developed to dispose of transuranic wastes from national defense programs. Both the wastes and the process of site development at this site are different from the DOE commercial nuclear waste program; WIPP is mentioned here for the sake of completeness.

The construction of the second commercial waste repository is scheduled to follow the first by about 3 years. To expand the number of possible sites available for a second repository, DOE has recently identified from a literature survey more than 200 crystalline rock bodies in the Appalachians, Adirondacks, and Lake Superior Precambrian shield that might contain suitable sites [Office of Crystalline Repository Development, 1983]. From these, a much smaller number will be selected for field investigation.

In addition, the U.S. Geological Survey, working in cooperation with most of the states involved, identified potential areas in the Basin and Range Province that could also be considered [Schneider and Trask, 1982, pp. 5-6; Bedinger et al., 1985a, b; Sargent and Bedinger, 1985]. Like the first repository, the second one ultimately will be chosen from three that have been thoroughly characterized, including an exploratory shaft. One or two of these could be candidates previously characterized but not chosen for the first repository.

### LIMITATIONS OF DRILLING

Because any repository below the water table will eventually become filled with water, all drill holes and shafts into it must be carefully sealed to minimize future groundwater circu-

This paper is not subject to U.S. copyright. Published in 1987 by the American Geophysical Union.

Paper number 6B5981.

1783  
1784  
1786  
see 7793

acquisition have been carried out at the NTS, along with detailed three-dimensional modeling. A broad range of resistivity, telluric profiling, and time and frequency domain electromagnetic measurements have also been made, with modeling follow-up to identify potential faults and other water-channeling structures in the Yucca Mountain block. These methods have proven particularly useful in mapping steep faults hidden by alluvium in surrounding valleys and pediments.

A natural seismicity network has been in place since 1979, and *P* wave residual studies to look for deep basement structures and magma reservoirs have been carried out utilizing underground nuclear tests from the northern and central parts of the NTS. Several reflection seismic studies have been carried out in the Yucca Mountain vicinity, but despite use of unusually rigorous field acquisition and processing procedures, the efforts were disappointing largely due to the extreme attenuation of seismic energy by the volcanic tuffs.

#### ISSUE OF SENSITIVITY OF GEOPHYSICAL METHODS

Table 1 shows most of the ways in which geophysical methods have been used at the various sites. All of these methods have been used at the Nevada Test Site, and most of them have been used at the Hanford site and the Paradox Basin. Less than half of the techniques have been used at the Deaf Smith County site: only reflection seismics, seismicity networks, borehole logging, and regional scale gravity/magnetics have been used in the Permian Basin as of this writing. Reflection seismic, borehole logging suites, VES data, and potential field geophysics are the only data acquired at the salt domes in the southeastern United States (M. Gibbons, personal communication, 1985).

Geophysical parameters being measured vary tremendously with the geologic and geohydrologic environment. The lithologic and structural features being sought vary greatly also, even within the present limited set of candidate sites for the first repository. It is not unreasonable that a sequence of geophysical surveys could be carried out that showed no significant anomalies yet missed a significant feature that would later be encountered in drilling or mining. A large brine pocket found at the WIPP site would be an example, though no electrical geophysical surveys, which might have found it, were carried out there. We must, therefore, be able to determine the sensitivity and resolving power of the methods listed in Table 1 and be able to answer such questions as what size and what kinds of inhomogeneities will they detect and at what distances? In order to meet the requirements of quality assurance programs, we need to know the size of geological features that might slip through the geophysical seine.

The penetration and resolution examples shown in column 3 of Table 1 are specific (and by no means complete) to problems being studied at the sites shown in Figure 1. They are nevertheless put here to provide some overall sense of the capabilities and limitations of geophysical methods in the disposal of high-level radioactive wastes. For each site, and each particular geologic/geohydrologic question needing answers, extensive computer modeling is required to ascertain the resolution of each method. This kind of detailed analysis, quite beyond the scope of this paper, is only summarized in Table 1. For further information, the reader is directed to other papers in this and other issues of the *Journal of Geophysical Research*.

Some specific comments about how each group of geophysical methods applies to the disposal problem of high-level radioactive wastes follows:

Regional scale gravity and magnetic methods can provide information about lithology and structure of the crystalline rocks underlying sedimentary sequences but usually can provide little information about the sedimentary layers themselves. Borehole gravity can give in situ densities for the overlying individual sedimentary layers, and three-component borehole magnetic tools can provide information on natural remanent magnetization and polarity reversals for stratigraphic correlation and dating purposes. These potential fields methods have proven especially helpful toward understanding what underlies the thick volcanic sequence at Yucca Mountain at the NTS [Snyder, 1981, Kane *et al.*, 1982], as well as in suggesting the structures underlying the bedded salts of the Paradox Basin in Utah [Hildenbrand and Kuchs, 1983], and the sediments overlying the Pasco Basin at the Hanford Reservation [Rockwell International, 1983].

Electrical geophysical methods used at the surface are of special interest because they can provide information on the presence of water or brine in the underlying rocks. In a salt environment the presence of brine is very significant, as it raises the question of whether the salt might be undergoing active dissolution. The Schlumberger method has worked well in investigating dissolution in the bedded salt in the Paradox Basin [Watts, 1982, 1983]. Electrical methods, however, cannot penetrate very far into a high-resistivity salt sequence, unless that sequence is interrupted by a solution feature or a fault. Newly developed time domain electromagnetic (TDEM) methods have identified conductors as deep as 1 km at the NTS. There is some indication that TDEM could be more effective in evaluating thick, highly resistive bedded salt units where galvanic current systems do not easily penetrate.

The magnetotelluric (MT) method, while useful in providing deep crustal resistivity information to supplement regional scale gravity and magnetics, has relatively poor resolution compared to other geophysical methods that have been used to study potential disposal sites, and this resolution gets worse with increasing depth. It is best used in deep layered-earth situations where adequate seismic data are not obtainable. Its maximum resolution under optimum conditions is five layers for the first 10 km of depth (W. D. Stanley, personal communication, 1985); MT has been used at the Hanford site [Rockwell International, 1979]. Audiofrequency magnetotellurics could be used at potential disposal sites, but the typical lowest frequency of about 7 Hz limits its penetration to less than 500 m or less, depending on the resistivity of the underlying rocks.

The telluric profiling method, an offshoot of the MT method, can resolve fault systems to great depths if they are large enough and conductive enough. The minimum target width that can be resolved (for a conductive target) is the dipole length, (typically 100–500 m) though conductive fracture zones narrower than this can be recognized readily enough. Below one or two dipole lengths depth, the conductor would have to be a minimum of one dipole length wide to be seen.

Standard borehole logging methods [Nelson *et al.*, 1982] are used for correlation purposes in layered sediments and volcanic rocks and also for identification of water-filled fractures and otherwise anomalous zones in crystalline rocks as well as salt. The neutron gamma method can do actual elemental identification and can effectively penetrate about a meter from the borehole wall. The log normal (single-electrode electrical) method can penetrate (on the average) about 75 cm, while most other tools can penetrate no more than 15–20 cm from the borehole at most. One additional logging tool, the



ultra-long-spaced electric log, can exceed the 75-cm limit but is not commonly used because of lower resolution.

New borehole techniques have been developed that hold great promise for providing crucial hydrologic information easily and rapidly. Tube waves are low-velocity, low-frequency acoustic waves generated by sources placed within the borehole that subsequently propagate along the borehole walls. Recent results by *Huang and Hunter* [1983] have shown that amplitude variations of tube waves can be used to identify fractures intersecting boreholes and can even be used to clarify whether a fracture is open to fluid flow.

Borehole gravity methods [*Hearst*, 1977; *Brown and Lautzenhiser*, 1982] are used almost routinely at the BWIP and NTS sites to map in situ densities and search for anomalous variations in porosity. Borehole radar, including azimuthal versions [*Wright and Watts*, 1983] and hole-to-surface and hole-to-hole tomographic methods have been developed largely to resolve fractures and fracture zones in crystalline rocks and salt. Computer modeling programs are finally on line that can provide quantitative answers to questions of feature resolution for most of these methods in most geologic environments.

Borehole-to-surface electrical methods, described by *Daniels* [1983a, b], can identify zones of high conductivity such as a brine pocket within a salt sequence as much as a kilometer away from a borehole. The maximum distance from a borehole that a conductive zone can be detected is about twice the borehole depth, with the proviso that the zone size be no less than a fifth of the source-target distance. Inhole radar systems have been developed that have successfully mapped fractures and impurities in three dimensions at distances of 500 m from the borehole in salt and up to 100 m from the borehole in crystalline rocks [*Nickel et al.*, 1985; *Wright and Watts*, 1983].

Heat flow measurements in boreholes at the NTS [*Sass*, 1982; *Sass and Lachenbruch*, 1982] have proven to be very sensitive in identifying vertical migration of water in the surrounding rocks because even a relatively small flow of water disturbs the normal thermal gradient. At the Paradox Basin the temperature data showed that if any water is moving vertically, the rate must be less than a few millimeters per year (*J. Sass*, written communication, 1982). Heat flow data of course provide information on recent volcanism and geothermal potential, which are potentially useful at the NTS and Hanford sites; at the Hanford site, no shallow heat sources have been detected in the primary target zone (*A. Tallman*, personal communication, 1985).

The thermal stress caused by the hot waste in the host rock will be important, especially for rocks other than salt. The thermal stress generated by the waste will be added to the in situ stress. These stresses must both be known if we are to model the complex hydrologic, mechanical, and thermal interactions that will take place around a repository as it heats up [*Lawrence Berkeley Laboratory*, 1979]. At both Yucca Mountain, Nevada, and Hanford, Washington, this problem has been addressed [*Ellis and Swolfs*, 1983; *U.S. Department of Energy*, 1982, pp. 54-58]. The safety as well as the constructibility (will the repository self-destruct as it is being filled with waste canisters?) of any site is strongly dependent upon satisfactory answers to these modeling questions. Hydrofrac techniques and laboratory stress measurements can provide parameters for the models, as well as direct experimental evidence.

Local seismicity studies like those at the NTS [*Schneider and Trask*, 1982, pp. 7-10; *Monfort and Evans*, 1982] are important, of course, in indicating which faults in an area may be

currently active. Microseismic networks are also extremely important in searching for dissolution in the vicinity of salt sites; one has been used to detect solution mining at a potash mine in the Paradox Basin. Seismic refraction methods can be used to search for magma chambers, and seismicity could play a supportive role in the positive identification of any such features if they are currently developing, such as the magma system at Mono Lakes, California. Teleseismic *P* wave residuals are useful in regional scale tectonics mapping, particularly in the search for magma-caused low-velocity zones. Resolution is very coarse, however, being on the order of the station spacing (typically a kilometer or more).

Remote sensing methods, particularly Landsat image processing, figure prominently in early phases of exploration because of their ability to provide large-scale structural information, some of which is unobtainable by conventional geological mapping. Recent studies in Wisconsin have shown that fractures in precambrian basement rocks have expression in overlying glacial till, and side-looking airborne radar (SLAR) is a primary tool being used in both Wisconsin and Connecticut to search for these hidden structures (*M. Ostrom*, personal communication, 1985; *S. Quarrier*, personal communication, 1985).

Seismic refraction methods, under optimum circumstances, can pinpoint a vertical offset in a horizontal sedimentary sequence as small as 1% of the depth. Under less-than-optimal circumstances, such as at the NTS, this precision may fall to 5-10% of the depth, or worse (*D. Dansereau*, personal communication, 1985).

Seismic reflection methods, though cost and labor intensive, are extremely helpful in mapping horizontal and subhorizontal sedimentary formations and in searching for discontinuities in them. There are serious difficulties attendant to using seismic reflection methods in certain environments, particularly volcanic rocks. Because of extreme signal attenuation problems, along with very large source-generated noise trains and extreme lateral velocity variations in near-surface rocks, recent attempts to map ash flow tuff units at the NTS using seismic reflection techniques have been unsuccessful: no reflected signals could be obtained [*McGovern*, 1983]. The resolution of seismic reflection methods, however, far exceeds that of surface electrical or seismic refraction methods in areas where sufficient return signal can be obtained.

#### QUALITY ASSURANCE

The primary use of geophysics is in the regional exploration stage although borehole geophysical methods and detailed surface studies will be useful in the site characterization stage. The potential also exists to use geophysical methods underground. During the exploration stage, candidate sites are being screened to determine which sites offer the best likelihood of success and which ones warrant the much larger investment involved in sinking a shaft and making further subsurface studies. This use of geophysics is similar to its applications in mining and hydrocarbon exploration, where initial conclusions from geophysical studies are tested by drilling and mining to provide the definitive answers. For a repository, however, some of the conclusions based on geophysical studies can never be tested and will have to stand on their own if they are a part of the DOE license application to the NRC.

Any studies that may be used to support a licensing application will have to show that they were conducted in compliance with NRC's requirements for a quality assurance (QA) program that adequately documents the method used and the procedures carried out in the data acquisition and interpreta-

tion. Under a QA program, all procedures used must be described in detail prior to the start of the work, and any changes in procedures must be carefully documented and justified, so that the licensers know which data were collected before and which after any changes were made. The written record must be so complete that a geophysicist peer would encounter no uncertainties regarding what was actually done in the field, how the equipment was calibrated, how the data were collected and processed, and how the interpretations were made.

Few exploration geophysical methods can be applied in a cut-and-dried manner but must instead be tailored to fit a complex, evolving problem. The QA requirement can be viewed as a unique challenge, as well as an opportunity for geophysicists to think carefully about their craft and to document it adequately. Apparently, the challenge can be met, but at considerable increase in the amount of attendant paperwork. The results, however, are clearly required for the licensing effort. The extra effort expended will also go a long way toward explaining the rationale behind the methods and decisions and should help justify the relatively large costs of geophysics conducted in the public domain.

*Acknowledgments.* This paper, especially Table 1, owes a great deal to the advice and experience of a number of geophysicists and geologists doing work related to radioactive waste disposal. These include Jeff Daniels, Frank Sentfle, Tom Hildenbrand, David Wright, Mahadeva Iyer, Frank Frischknecht, Al Rogers, Don Hoover, W. Dal Stanley, Danny Dansereau, Jerry Wermund, Meredith Ostrom, Sid Quarrier, Ann Tallman, James Hileman, Mike Gibbons, and two anonymous reviewers.

#### REFERENCES

- Bedinger, M. S., K. A. Sargent, and J. E. Reed, Geologic and hydrologic characterization and evaluation of the basin and range province relative to the disposal of high-level radioactive waste, Part I, Introduction and guidelines, *U.S. Geol. Surv. Circ.*, 904A, 67 pp., 1985a.
- Bedinger, M. S., K. A. Sargent, and B. T. Brady, Geologic and hydrologic characterization and evaluation of the basin and range province relative to the disposal of high-level radioactive waste. Part III, Geologic and hydrologic evaluation, *U.S. Geol. Surv., Circ.*, 904C, 72 pp., 1985b.
- Brown, A. R., and T. V. Lautzenhiser, The effect of dipping beds on a borehole gravimeter survey, *Geophysics*, 47, 25-30, 1982.
- Caggiano, J. A., and D. W. Duncan (Eds.), Preliminary interpretation of the tectonic stability of the reference repository location, Cold Creek Syncline, Hanford site, *Rep. RHO-BW-ST-19P*, Rockwell Int., Energy Syst. Group, Hanford, Wash., 1983.
- Daniels, J. J., Evaluation of nuclear waste sites with hole-to-surface resistivity measurements, in *Proceedings of the OECD Workshop on Geophysical Investigations in Connection with Geological Disposal of Radioactive Waste*, Ottawa, Canada, 1982, pp. 235-258, Organization for Economic Cooperation and Development, Nuclear Energy Agency, Paris, 1983a.
- Daniels, J. J., Hole-to-surface resistivity measurements, *Geophysics*, 48, 87-97, 1983b.
- Ellis, W. L., and H. S. Swolfs, Preliminary assessment of in-situ geomechanical characteristics in drill hole USW G-1, Yucca Mountain, Nevada, *U.S. Geol. Surv. Open File Rep.*, 83-401, 17 pp., 1983.
- Healey, J. H., M. D. Hickman, M. D. Zoback, and W. L. Ellis, Deep borehole stress measurements at the Nevada Test Site, *Eos Trans. AGU*, 63, 1099-1100, 1982.
- Hearst, J. R., Estimation of dip and lateral extent of beds with borehole gravimetry, *Geophysics*, 42, 990-994, 1977.
- Hildenbrand, T. G., and R. P. Kuchs, Regional magnetic and gravity features of the Gibson Dome area and surrounding region, Paradox Basin, Utah, a preliminary report, *U.S. Geol. Surv. Open File Rep.*, 83-359, 35 pp., 1983.
- Huang, C. F., and J. A. Hunter, The tube-wave method of estimating in-situ rock fracture permeability in fluid-filled boreholes, in *Proceedings of the OECD Workshop on Geophysical Investigations in Connection with Geological Disposal of Radioactive Waste*, Ottawa, Canada, 1982, pp. 173-188, Organization for Economic Cooperation and Development, Nuclear Energy Agency, Paris, 1983.
- Kane, M. F., G. D. Bath, D. B. Snyder, J. G. Rosenbaum, H. W. Oliver, D. A. Ponce, and D. L. Healey, Gravity and magnetic studies in the region of the Nevada Test Site, *Eos Trans. AGU*, 63, 1099, 1982.
- Lawrence Berkeley Laboratory, Geotechnical assessment and instrumentation needs for nuclear waste isolation in crystalline and argillaceous rocks, *Symposium Proceedings*, July 16-20, 1978, *LBL Rep. 7096*, 218 pp., Berkeley, Calif., 1979.
- McGovern, T. F., An evaluation of seismic reflection studies in the Yucca Mountain area, Nevada Test Site, with an introduction by L. N. Pankratz and H. D. Ackermann, *U.S. Geol. Surv. Open File Rep.*, 83-912, 57 pp., 1983.
- Monfort, M. E., and J. R. Evans, Teleseismic studies of the earth's crust and upper mantle in southern Nevada, *Eos Trans. AGU*, 63, 1099, 1982.
- National Academy of Sciences, A study of the isolation system for geologic disposal of radioactive waste, report, 345 pp., Waste Isolation Syst. Panel, Board on Radioact. Waste Manage., Comm. on Phys. Sci., Natl. Res. Council, Washington, D. C., 1983.
- Nelson, P. H., K. A. Magnusson, and R. Rachiele, Application of borehole geophysics at an experimental waste storage site, *Geophys. Prospect.*, 30, 910-934, 1982.
- Nickel, H., F. Sender, R. Thierbach, and H. Weichart, Exploring the interior of salt domes from boreholes, *Geophys. Prospect.*, 31, 131-148, 1983.
- Office of Crystalline Repository Development, A national survey of crystalline rocks and recommendations of regions to be explored for high-level radioactive waste repository sites, *Rep. OCRD-1*, 110 pp. Battelle Mem. Inst., Columbus, Ohio, 1983.
- Rockwell International, Geological studies of the Columbia Plateau, Appendix E, Magnetotelluric Studies, *Rep. RHO-BW1-ST-4*, 41 pp., Hanford, Wash., 1979.
- Rockwell International, Preliminary interpretation of the tectonic stability of the reference repository location, Cold Creek Syncline, Hanford site, *Rep. RHO-BW-ST-19P*, 136 pp., Hanford, Wash., 1983.
- Roseboom, E. H., Jr., Disposal of high-level nuclear waste above the water table in arid regions, *U.S. Geol. Surv. Circ.*, 903, 28 pp., 1983.
- Sargent, K. A., and M. S. Bedinger, Geologic and hydrologic characterization and evaluation of the basin and range province relative to the disposal of high-level radioactive waste, Part II, Geologic and hydrologic characterization, *U.S. Geol. Surv. Circ.*, 904B, 72 pp., 1985.
- Sass, J. H., Hydrologic implications of preliminary heat-flow data from the Nevada Test Site, *Eos Trans. AGU*, 63, 1099, 1982.
- Sass, J. H., and A. H. Lachenbruch, Preliminary interpretation of thermal data from the Nevada Test Site, *U.S. Geol. Surv. Open File Rep.*, 82-973, 30 pp., 1982.
- Schneider, R., and N. J. Trask, U.S. Geological Survey research in radioactive waste disposal—Fiscal year 1980, *U.S. Geol. Surv. Open File Rep.*, 82-509, 110 pp., 1982.
- Scott, R. B., R. W. Spengler, S. Diehl, A. R. Lappin, and M. P. Chornack, Geologic character of tuffs in the unsaturated zone at Yucca Mountain, southern Nevada: Role of the unsaturated zone in radioactive and hazardous waste disposal, pp. 289-335, Butterworths, Stoneham, Mass., 1983.
- Smedes, H., The national program for isolating high-level nuclear waste, *Underground Space*, 6, 220-228, 1982.
- Snyder, D. B., Gravity interpretation of Yucca Mountain, Nye County, Nevada, and its implications for southern Nevada structure, *Eos Trans. AGU*, 62, 1039, 1981.
- U.S. Department of Energy, *Proceedings of the 1982 National Terminal Waste Storage Meeting*, pp. 54-58, Battelle Project Management Division, Columbus, Ohio, 1982.
- U.S. Department of Energy, Draft environmental assessment, Davis Canyon site, Utah, *Rep. DOE/RW-0010*, 1079 pp., Washington, D. C., 1984a.
- U.S. Department of Energy, Draft environmental assessment, Yucca Mountain site, Nevada research and development area, Nevada, *Rep. DOE/RW-0012*, 945 pp., Washington, D. C., 1984b.
- U.S. Department of Energy, Draft environmental assessment, Richton dome site, Mississippi, *Rep. DOE/RW-0013*, 955 pp., Washington, D. C., 1984c.
- U.S. Department of Energy, Draft environmental assessment, Deaf Smith County site, Texas, *Rep. DOE/RW-0014*, 1104 pp., Washington, D. C., 1984d.
- U.S. Department of Energy, Draft environmental assessment, Refer-

thin  
nickel

1:750,000

Saltus, 1988, Bouguer grav anom map Nev.  
Saranov, V. 1957, Geophys, V. 22, n. 2, p. 359-383.

Chapter title INTRODUCTION etc

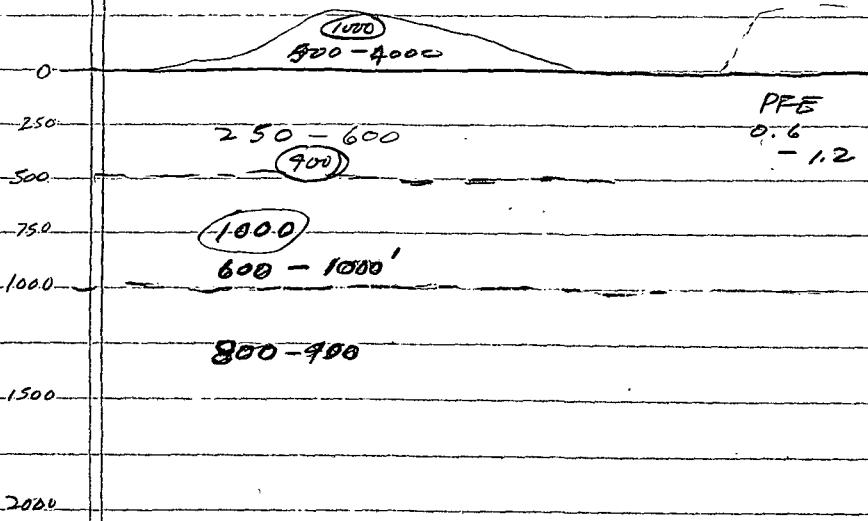
Sub Chapter Principal Sub Chapter

W

500'  
C, D, E @ 152m

200'  
A, B, D @ 60m

305'  
B @ 1000



## Introduction to Special Section on Geophysical Investigations of Proposed Radioactive Waste Disposal Sites

H. W. OLIVER

*Office of Mineral Resources, U.S. Geological Survey, Menlo Park, California*

A symposium on "Geophysical Investigations of Proposed Radioactive Waste Disposal Sites" was held at the Fall Meeting of the American Geophysical Union, December 13, 1982. Since then, five of the papers presented at the symposium have been published in the *Journal of Geophysical Research* and an additional six papers are included in this issue. Three of the current papers involve geophysical research at Yucca Mountain, Nevada; two papers are on subsurface structure and fracturing of the Strath-Halladale granite in northern Scotland, a prime candidate for rad waste storage in the United Kingdom; and a general paper is included on the application of various geophysical methods for characterizing all the potential storage sites in the United States under consideration by the U.S. Department of Energy.

In 1982, the following nine sites in the United States (Figure 1) were under consideration by the U.S. Department of Energy for the first U.S. repository of high-level radioactive waste (HLW). The host rock at each site is noted in parentheses (from NW to SE): Hanford, Washington (Miocene basalt flows); Yucca Mountain, Nevada (Tertiary tuff); Davis Canyon, Utah, (bedded salt); Lavender Canyon, Utah (bedded salt); Deaf Smith, Texas (Permian bedded salt); Swisher County, Texas (Permian bedded salt); Vacherie dome, Louisiana (domal salt); Richton dome, Mississippi (domal salt); and Cypress Creek dome, Mississippi (domal salt)

Geologic studies of some potential granite, argillite, and salt sites have been made in Europe by the Commission of the European Communities and the British Geological Survey [Milodowski and Wilmot, 1983; Mather, 1984; N. R. Brereton, written communication, 1985]. The problems associated with long-term contamination by radionuclides are not so severe in Europe because of the United Kingdom and French decisions in 1981 to remove and recycle plutonium from British-generated HLW, thus converting the HLW to an intermediate level product. See Krugman and von Hippel [1980] for a discussion of this problem.

Subsequent to the 1982 American Geophysical Union symposium, the number of potentially acceptable sites for the first HLW repository in the United States was reduced to three: Hanford, Yucca Mountain, and Deaf Smith (Figure 1) [Associated Press, 1986]. In addition, the Waste Isolation Pilot Plant (WIPP) site in New Mexico (Figure 1) has been chosen as the U.S. National Repository for the Department of Defense HLW [Eos, *Transactions of the American Geophysical Union*, 1984]. Intensive subsurface and surface "characterizations" of these sites are presently in progress,

This paper is not subject to U.S. copyright. Published in 1987 by the American Geophysical Union.

Paper number 7B1040.

and the most important scientific results are being reported in appropriate journals. For example, five of the papers presented in the 1982 symposium have already been published in this Journal. These papers present (1) gravity, magnetic, and resistivity evidence for a buried Tertiary intrusion at Wahmonie just east of Yucca Mountain [Ponce, 1984], (2) interpretation of new gravity data over the Yucca Mountain site showing the site to be located over the east edge of a large structural depression in the Paleozoic bedrock [Snyder and Carr, 1984], (3) hydraulic fracturing stress measurements in two 2000-m-deep wells in Yucca Mountain; the results yielded values of the least horizontal stress that are considerably lower than the vertical principal stress, indicating a normal faulting stress regime [Stock *et al.*, 1985], (4) laboratory measurements on the effect of temperature on the permeability of possible tuffaceous host rocks at Yucca Mountain [Moore *et al.*, 1986], and (5) a study of the paleomagnetic properties of the Tiva Canyon and Topopah Spring tuffs at Yucca Mountain [Rosenbaum, 1986]. The symposium paper presented by Oliver *et al.* [1982] on characterization of Yucca Mountain has since been expanded into a summary document [U.S. Geological Survey, 1984]. Also, the symposium paper presented by Mooney *et al.* [1982] is being published in a U.S. Geological Survey (USGS) bulletin on radioactive waste studies [Ackermann *et al.*, 1987]. Much of the regional gravity and aeromagnetic data in southern Nevada reported in the abstract by Kane *et al.* [1982] is being released by Hildenbrand *et al.* [1987] in a USGS bulletin. For a review of the geophysical methods that have been applied to the study of the Yucca Mountain site, see Oliver [1984].

In this special section on "Geophysical Investigations of Proposed Radioactive Waste Disposal Sites," the following six papers are included:

1. J. C. Wynn and E. H. Roseboom, The role of geophysics in identifying and characterizing sites for high-level nuclear waste repositories.
2. N. R. Brereton, T. J. McEwen, and M. K. Lee, Fluid flow in crystalline rocks: Relationships between groundwater spring alignments and other surface lineations at Aetnabreac, United Kingdom.
3. M. K. Lee, Geophysical investigations in the Strath Halladale-Aetnabreac district (northeast Scotland) in relation to radioactive waste disposal.
4. S. Sinnock, Y. T. Lin, and J. P. Brannen, Preliminary bounds on the expected postclosure performance of the Yucca Mountain repository site, southern Nevada.
5. A. L. Ramirez and W. D. Daily, Evaluation of alterant geophysical tomography in welded tuff.
6. W. D. Daily, W. Lin, and T. A. Buschek, Hydrological properties of Topopah Spring tuff: Laboratory measurements.

Table 2.1-1. Regional Gravity Maps of Various Areas within the Regional Study Area (Figure 2.1-1)

Description	Scale	Reference
Bouguer and residual gravity map of Southern Great Basin	1:2,500,000	Hildenbrand et al., 1988, Fig. 2.8 & 2.11
Bouguer gravity map of Nevada	1:750,000	Saltus, 1988a
Bouguer gravity map of California	1:750,000	Oliver et al., 1980
Residual gravity map of California	1:750,000	Roberts et al., 1981
Residual gravity map of Nevada	1:1,000,000	Saltus, 1988b
Bouguer gravity map of Death Valley Sheet	1:250,000	Healey et al., 1980b
Bouguer gravity map of Goldfield	1:250,000	Healey et al., 1980a
Bouguer gravity map of Caliente Sheet	1:250,000	Healey et al., 1981
Bouguer gravity map of Las Vegas Sheet	1:250,000	Kane et al., 1979
Complete Bouguer gravity map of NTS	1:100,000	Healey et al., 1988c
Isostatic residual gravity map of NTS	1:100,000	Ponce et al., 1988
Residual gravity map of Yucca Mt. and vicinity	1:48,000	Snyder & Carr, 1982

Table 2.2-1. Aeromagnetic surveys all or partly within the Yucca Mountain Site Area and vicinity (refer to Figure 2.2-1)<sup>a</sup>

NEVADA (see Erwin et al., 1980; and Hill, 1986)									
Area name	Year flown	Contractor	Elev (ft)	Spacing (mi)	Direction	Scale	Gradient Removed	Digital	Reference
1 Topopah Spring	1961	USGS	8,000 b	1/2	E-W	1:62,500	no	no	Boynton & Vargo, 1963
2 Goldfield	1967	LKB	9,000 b 15,000 b	1	E-W	1:250,000	no	no	USGS, 1971 <sup>b</sup>
2 Goldfield	1967	LKB	9,000 b	1	E-W	1:62,500	no	n.a.	USGS, 1967 <sup>b</sup>
3 Timber Mtn.	1977	AG	400 d	1/4	E-W	1:62,500	IGRF		USGS, 1979
4 Lathrop Wells	1978	Aero	400 d 1,000 d	1/4-1/2 1/4-1/2	E-W N-S	1:62,500	IGRF	yes	USGS, 1978
5 NURE (Death Valley)	1979	GEO-LIFE	400 d	1	N-S	1:500,000	IGRF	yes	DOE, 1979
6 Yucca Mtn.	1982	HLQEB	400 d	1/4	N-S	1:62,500	IGRF	n.a.	USGS, 1984

<sup>a</sup>Key: Aero Aero Service  
 AG Applied Geophysics Inc.  
 b barometric  
 d drape  
 E east  
 HLQEB High-Life QEB  
 IGRF International Geomagnetic Reference Field  
 LKB Lockwood, Kessler & Bartlett, Inc.  
 N north  
 n.a. not available  
 NURE National Uranium Resource Evaluation  
 S south  
 USGS United States Geological Survey  
 W west

<sup>b</sup>USGS (1971) and USGS (1967) were reports on the same survey at different compilation scales.

Table 2.3-1. Geoelectric Investigations on Yucca Mountain

A.. Investigations with depth control provided by multi-frequency or variable-spacing source-receiver configurations.  
(The locations of lines E1-E13 are shown on Fig. 2.3-2.)

<u>METHOD</u>	<u>APPROXIMATE DEPTH RANGE</u>	<u>LOCATION</u>	<u>REMARKS</u>	<u>REFERENCE</u>
Schlumberger soundings (max. electrode separation 1,200 m)	1 - 600 m	14 soundings variably spaced along Lines E1, E2 of Figure 2.3-2; 14 km of profile	1-D modeling contoured to show resistivity contrasts related to faults and horizontal contrasts indicating variation in pore-water lithology with depth	Senterfit et al., 1982
Dipole-dipole resistivity/IP (61-m dipoles)	60 - 180 m	Lines E3, E4, E5 of Figure 2.3-2; 4.4 km of profile	2-D models incorporating topography show resistivity contrasts related to faults and lithologic variation	Smith and Ross, 1982
Dipole-dipole resistivity/IP (152-m dipoles)	150 - 450 m	Lines E6, E7, E8 of Figure 2.3-2; 8.8 km of profile	2-D models as above	Smith and Ross, 1982
Dipole-dipole resistivity/IP (305-m dipoles)	300 - 930 m	Lines E9, E11, E12 of Figure 2.3-2; 16.4 km of profile	2-D models as above except models for lines E11 and E12 do not incorporate topography	Smith and Ross, 1982; Ross and Lunbeck, 1978
EM soundings (time-domain, central receiver)	200 - 1,200 m	Lines E10, E13 of Figure 2.3-2 (250-m spacings); 3.9 km of profile	1-D modeling composited to show fault-controlled lateral resistivity contrasts as well as lithology and pore-water controlled horizontal contrasts.	Frischknecht and Raab, 1984

Table 2.3-1. Geoelectric Investigations on Yucca Mountain (continued)

<u>METHOD</u>	<u>APPROXIMATE DEPTH RANGE</u>	<u>LOCATION</u>	<u>REMARKS</u>	<u>REFERENCE</u>
Borehole-to-Surface DC resistivity 1981	30 - 300 m	an area of 300 m x 500 m just NW of drillhole UE25b-1H; sources in drillholes UE25 a#4, a#5, a#6; dipole receivers on 25 - 50 m grid	apparent resistivity contoured; 3-D ellipsoidal body modeled	Daniels and Scott, 1981
Audiomagnetotelluric soundings (6-250 Hz)	200 - 2,000 m	4 soundings (#'s 100 - 400) along 1-km profile	1-D and 2-D modeling shows general consistency with time-domain interpretation above	Unpublished data, USGS, 1981
Magnetotelluric soundings (.001-10 Hz)	2 - 20 km	soundings roughly along lines E1 and E2 of Figure 2.3-2	1-D modeling shows variations in conductance of upper crust related to variations in thickness and lithology of volcanic and sedimentary rocks; also a mid-crustal low resistivity layer, apparently related to crustal fluids and enhanced temperature.	Furgerson, 1982, and unpublished contract report, USGS, 1979



Table 2.3-1. Geoelectric Investigations on Yucca Mountain (continued)

B. Profile/mapping investigations with equivocal depth control. (Lines are not shown on Fig. 2.3-2.)

<u>METHOD</u>	<u>APPROXIMATE DEPTH RANGE</u>	<u>LOCATION</u>	<u>REMARKS</u>	<u>REFERENCE</u>
"Slingram" (dual-loop EM profiling; 222- 3555 Hz, fixed separation)	8-150 m	16.6 km of profile	lateral apparent resistivity contrasts indicate variations in alluvial thickness and bedrock faults	Flanigan, 1981
VLF (magnetic variation of fields related to 18.6 kHz navigation beacon)	10-60 m	4 km profile, parallel to Slingram profile (see above) over alluvium	results ambiguous due to insufficient penetration in conductive overburden	Flanigan, 1981
41 TURAM (magnetic variation of fields from EM line-source; 900 m source)	20-200 m	1.1 km of profile; over alluvium-covered fault detected by Slingram profile	results were ambiguous due to insufficient penetration or signal resolution	Flanigan, 1981
MAGNETOMETRIC (magnetic variation of field from 1 Hz line-source)	200-2,000 m	2 lines; 4.2 km of profile over alluvium-covered fault	identified apparent resistivity contrast of fault	Fitterman, 1982
Telluric-ratio (.025-.05 Hz, 500-m dipoles)	1 to 10 km	2 lines; 30 km of profile across northern part of Fortymile Wash	detected apparent resistivity variations related to bedrock faults	Hoover et al., 1982c

Table 2.5-1. Existing Seismic Reflection Data and Past Surveys

---

Shallow Crustal (0-2 sec) Profiles

1. Crater Flat/Amargosa Desert - high-resolution Mini-Sosie reflection profiles acquired and processed by the USGS (USGS, 1988)  

Quality - fair to good  
Objectives - image faults/fault offsets in Quaternary alluvium  
Results - partly to fully successful imaging of fault offsets
2. Death Valley - high-resolution Mini-Sosie reflection line (L. Serpa, University of New Orleans, personal communication, 1988)
3. Yucca Mountain - various high-resolution profiles commissioned by the USGS discussed by McGovern et al. (1983)

Intermediate Crustal (0-5 sec) Profiles

4. Mid Valley/Nevada Test Site - land air-gun profiling of the upper 3-5 sec of the crust (McArthur and Burkhard, 1986)  

Quality - good to excellent  
Objectives - map depth to Paleozoic basement in Tertiary basins  
Results - successful imaging of basin fill and subhorizontal detachment faults
5. Yucca Flat/Nevada Test Site - land air-gun profiling of the upper 3-5 sec of the crust (N. Burkhard, personal communication, 1988)  

Quality - good to excellent  
Objectives - map depth to Paleozoic basement in Tertiary basins  
Results - successful imaging of basin fill and subhorizontal detachment faults
6. Frenchman Flat/Nevada Test Site - land air-gun profiling of the upper 3-5 sec of the crust (N. Burkhard, personal communication, 1988)  

Quality - good to excellent  
Objectives - map depth to Paleozoic basement in Tertiary basins  
Results - successful imaging of basin fill and subhorizontal detachment faults
7. Seisdata speculative lines - obtained with vibroseis and explosive sources
  - a. Las Vegas shear zone (Lines 8 and 8a of Wasatch Cordilleran hingeline reconnaissance survey)  

Quality - poor to fair  
Objectives - map Tertiary basins for hydrocarbon exploration  
Results - successfully obtained reflections from only the upper 1 sec

Table 2.5-1. Existing Seismic Reflection Data and Past Surveys (continued)

- 
7. Seisdata speculative lines - obtained with vibroseis and explosive sources (continued)
    - b. Pahrump Valley (Lines 12 and 17 of Sandy speculative survey)
  8. Geophysical Service Inc. speculative lines - obtained with vibroseis and explosive sources
    - a. Big Smokey Valley, Nevada
    - b. Monitor Valley, Nevada
    - c. Railroad Valley, Nevada
    - d. Tikaboo Valley, Nevada

for a-d:

Quality - poor to excellent

Objectives - image Tertiary basins for hydrocarbon exploration

Results - variable success in imaging sedimentary fill of Tertiary basins

9. Other speculative data - unknown source types
  - a. White River Valley, Nevada
  - b. Garden Valley, Nevada

Quality - unknown

Objectives - image Tertiary basins for hydrocarbon exploration

Results - unknown

#### Deep Crustal (0-15 sec) Profiles

10. Amargosa Desert near Beatty and Lathrop Wells - deep crustal Vibroseis and explosive feasibility study (Brocher et al., 1989)

Quality - good to excellent

Objectives - image entire crust down to the Moho

Results - successful imaging of all portions of the crust

11. Death Valley/SW Amargosa Desert/S. Pahrump Valley - deep crustal Vibroseis survey by COCORP (Serpa et al., 1988)

Quality - poor to fair

Objectives - image entire crust down to the Moho

Results - partly successful in mapping mid- to lower crustal structure

---

Editorial 2297

## SPECIAL INVITED PAPER

History of geophysical technology through advertisements in *GEOPHYSICS*,  
*R. E. Sheriff* 2299

## INVITED PAPERS

The effectiveness of offshore 3-D seismic surveys: Case histories,  
*P. S. Horvath* 2411

Fifty years of case histories, *R. W. Kettle* 2431

The present state of seismic data acquisition: One view, *S. J. Laster* 2443

Seismic data processing: Current industry practice and new directions,  
*P. S. Schultz* 2452

Migration and inversion of seismic data, *R. H. Stolt and A. B. Weglein* 2458

A guide to the current uses of vertical seismic profiles, *M. L. Oristaglio* 2473

Recent advances in rock physics, *D. P. Yale* 2480

Low-frequency electrical properties, *G. R. Olhoeft* 2492

Well logging: A 25-year perspective, *D. D. Snyder and D. B. Fleming* 2504

Physical characterization of rock masses using borehole methods, *A. V. Dyck and  
R. P. Young* 2530

A simple parametric model for the electromagnetic response of an anomalous  
body in a host medium, *G. F. West and R. N. Edwards* 2542

Applications of gravity and magnetic surveys: The state of the art in 1985,  
*N. R. Paterson and C. V. Reeves* 2558

Remote sensing: A geophysical perspective, *K. Watson* 2595

The analysis of multichannel airborne gamma-ray spectra, *R. L. Grasty,  
J. E. Glynn, and J. A. Grant* 2611

Geotechnical and groundwater geophysics, *T. L. Dobecki and P. R. Romig* 2621

Geophysics in Australian mineral exploration, *R. J. Smith* 2637

State of the art geophysical exploration for geothermal resources, *P. M. Wright,  
S. H. Ward, H. P. Ross, and R. C. West* 2666

Table of Contents continued on p. 2296

Stratigraphic, petrographic and structural evidence suggest that three distinct tectono-stratigraphic terranes in SW Alaska are related as co-genetic elements of a Mesozoic NW-facing volcanic arc complex. From SE to NW, the Kulukak, Togiak, and Goodnews terranes represent back-arc, volcanic arc, and forearc environments, respectively, of an ensimatic volcanic arc developed over a SE-dipping subduction zone during Early Jurassic through Early Cretaceous time. The Kulukak back-arc terrane consists of more than 5 km of Middle to Upper Jurassic volcanogenic turbidites, deposited as prograding submarine fans across a SE-dipping paleoslope. The Togiak volcanic arc terrane encompasses predominantly andesitic volcanic and volcanoclastic rocks of Early Jurassic through Early Cretaceous age. Interbedded shallow marine sedimentary rocks occur through most of the section. The Goodnews forearc terrane is composed of a varied assemblage of Lower and Upper Paleozoic and Mesozoic rocks. Where exposed on the coast, it consists of fault-bounded packets of mafic volcanic, volcanoclastic and intrusive rocks, and serpentinized ultramafic rocks. The degree of metamorphism varies between each packet. Occurrences of lawsonite-bearing mafic rocks and structurally associated ultramafic rocks strongly support interpretation of this terrane as a subduction complex. Deformational episodes of pre-Early Cretaceous and early Late Cretaceous ages are recorded in each terrane. The Late Cretaceous event, one of predominantly northwestward structural vergence, coincides with the juxtaposition of Kibuck Precambrian crystalline terrane against the NW edge of the Goodnews subduction complex.

T3-2-A-5

#### OPHIOLITE ZONES AND BLUESCHIST BELTS MARK MAJOR PLATE BOUNDARIES IN CHINA

Zhang, Zh.M., Liou, J.C. and Coleman, R.C.  
(Dept. Geology, Stanford University,  
Stanford, CA 94305)

China is contained mainly within the Eurasian plate but the margins of the Indian and Philippine Sea plates are involved in the Himalayas and the Coastal Range of Taiwan respectively. Within the Eurasian plate, the Cathaysian paleoplate is separated from the Angaraian paleoplate by the Zunggar-Hegen geosuture which contains Paleozoic ophiolite and rare blueschists. The three microplates of the Cathaysian paleoplate consist of Precambrian cratons and/or Phanerozoic accretionary fold belts. These coalesced Precambrian cratons now reveal 4 to 5 stages of intense orogeny before basement consolidation. The Paleozoic to Cenozoic accretionary fold belts of China can be correlated with similar events now found in the west-Pacific-, Andean-, and Atlantic type active continental margins. Ophiolites occupying many of these tectonic zones provide evidence for the age and igneous history of oceanic crust formed during this period. The presence of blueschist in many of these Chinese geosutures reveals evidence of large scale subduction and tectonic exhumation during consolidation of the Eurasian plate. Cenozoic collision of the Eurasian-Indian plates produced the uplift and deformation of the Himalayas, strongly influencing the tectonics of Western China. In contrast, Mesozoic-Tertiary evolution of eastern China is typical basin-range geology with development of deep sedimentary basins along with calc-alkaline plutonic and volcanic activity produced by thin-skinned tectonics and high heat flow. Tectonic evolution of China is complicated and the presence of ophiolites and blueschist in Proterozoic to Tertiary convergent boundaries provides evidence of an extremely mobile history of plate movements in China.

T3-2-A-6

#### ON THE NORTHERN BOUNDARY OF GONDWANALAND IN SE ASIA

Chi-yuen Wang (Department of Geology and Geophysics, University of California, Berkeley, CA 94720)

Lung-song Chan (Department of Geology and Geophysics, University of California, Berkeley, CA 94720)

The Ailao Shan - Red River fault zone in western Yunnan, along which numerous bodies of ultramafic rocks and glaucophane schists outcrop, is considered by some as part of an ancient suture zone that joined Eurasia and Gondwanaland in the late Mesozoic. Selsotectonic studies, however,

indicated sinistral movements since as early as the Quaternary, in reverse direction to the earlier movements inferred from the suture zone model. Oriented rock samples were collected from the upper Triassic redbed south of the fault zone for paleomagnetic studies. The results of the thermal demagnetization experiment are most simply interpreted as having reversed polarity and a virtual geomagnetic north pole at 39°N, 327°E, with alpha-95 equal to 7.1°. A nominal interpretation is that the redbed site moved 59° northward and rotated 77° counterclockwise when it arrived. Similar inferences were made for southern Tibet from paleomagnetic studies of rocks of similar age. Although many other interpretations are possible and much more extensive studies need to be made, the present data are supportive of the hypothesis that the western Yunnan, the southern Tibet, and maybe all of the SE Asia were part of Gondwanaland in the late Paleozoic; separation occurred in the early Mesozoic, and collision with Eurasia in the late Mesozoic.

T3-2-A-7

#### INVESTIGATIONS OF THE SLATE ISLANDS CRATER

M. E. Bengtson and R. P. Meyer  
(Geophysical and Polar Research Center,  
Department of Geology and Geophysics,  
University of Wisconsin, Madison, WI 53706)

Recent geophysical studies of the Slate Islands of Canada in northernmost Lake Superior have correlated observations of shock structures, cratering, and faulting with lowered seismic velocity under the crater due to brecciation at depth and consistent with intense deformation. We are attempting to determine not only the geophysical signature of the Slate Islands complex, but also general diagnostics for the presence of cratering.

A survey of the crater area (defined by an irregular arcuate bathymetric rise) is now nearly complete. A close-orbit aeromagnetic survey (1000-yd spacing, 425 m above lake level) and a set of marine magnetic and high-resolution 3.5 kc bottom and subbottom profiles taken under flight lines have shown several short wavelength anomalies on the east side of the islands. The sources of these anomalies appear to be 1/2 to 1 km below lake level, and none seem to have any bathymetric expression. To the west, a longer wavelength anomaly trending NW-SE has been delineated, which correlates well with a previously predicted igneous-sedimentary contact.

The islands seem to be centered about a roughly defined arcuate magnetic high. Digitally-recorded marine refraction and reflection records show large thicknesses (over 1 km) of a 3.5 km/sec layer underlain by a 5.5 km/sec refractor outside the crater. Inside the crater rim, the 3.5 km/sec layer is absent; here only a 4.8 km/sec refractor lying directly beneath unconsolidated sediments has been detected. This 4.8 km/sec refractor probably represents a brecciated zone of the 3.5 km/sec refractor.

T3-2-A-8

#### Nd and Sr ISOTOPIC EVIDENCE ON THE CRUSTAL STRUCTURE AND COMPOSITION OF THE NORTHERN GREAT BASIN

G. Lang Farmer and Donald J. DePaolo (Department of Earth and Space Sciences, University of California, Los Angeles, California 90024)

Two major discontinuities in the composition of the lower crust of the Northern Great Basin can be recognized from Nd and Sr isotopes in Mesozoic and Tertiary granites in a west-to-east traverse from N. California to Utah. The first, in east-central Nevada, is approximately coincident with the trace of the Roberts Mt. Thrust and the prethrusting facies transition between eu- and miogeosyncline. Here an abrupt decrease in  $\epsilon_{Nd}$  (-6 to -13) and increase in  $\epsilon_{Sr}$  (+40 to +150) marks the Paleozoic continental edge and the western limit of Precambrian basement today. The basement edge does not correspond to  $f_{Sm} = 0.706$  at the latitude, but would be described by  $f_{Sm} \approx 0.708$ .

The second boundary occurs  $\geq 50$  km west of the Wasatch hinge line in western Utah and is marked by a decrease in  $\epsilon_{Sr}$ , but with no accompanying shift in  $\epsilon_{Nd}$ . The boundary between Areas I and II Pb (Zartman, 1974) also corresponds to the drop in  $\epsilon_{Sr}$ . This is interpreted as marking the western limit of granulite-facies (low Rb, U) lower crust associated with the stable craton.

The basement in the region between the two boundaries is the same age as that to the immediate east but lacks Rb-U-depleted lower crust. Both appear to be mixtures of Archean (~2.8  $\epsilon$ ) and Proterozoic (1.8  $\epsilon$ ) crust, in contrast to the uniform-age crust (1.8  $\epsilon$ ) in

Colorado. The origin of the boundary between depleted and undepleted lower crust is problematical, but could have resulted from lateral variation of metamorphic grade in the orogenic episode at ~1.6  $\epsilon$  which affected all of the southwest U.S. Alternatively, an original depleted lower crust could have been destroyed during upper Proterozoic rifting. In either case, thick, undepleted basement remaining in NE Nevada after rifting, in conjunction with thermal blanketing by sediments, could have provided sufficient radioactive heating to cause the Mesozoic metamorphism seen in the core-complexes of the eastern Great Basin. Geochemical information on crustal structure must be integrated with geophysical studies to reconstruct the thermo-chemical evolution of the crust.

T3-2-A-9

#### GRAVITY INTERPRETATION OF YUCCA MOUNTAIN, NEVADA COUNTY, NEVADA AND ITS IMPLICATIONS FOR SOUTHERN NEVADA STRUCTURE

D. B. Snyder, (U.S. Geological Survey, Menlo Park, CA 94025)

The Miocene tuffs of Yucca Mountain are being considered as a repository for high-level nuclear wastes by the Department of Energy. Three-dimensional modeling based on data from 1350 gravity stations indicates tuff thicknesses between 1000 and 3500 m near the proposed repository. Isostatic gravity residuals ( $\rho = 2.67 \text{ g/cm}^3$ ,  $T = 25 \text{ km}$ ,  $\Delta\rho = 0.4 \text{ g/cm}^3$ ) with a Bouguer reduction density of  $2.00 \text{ g/cm}^3$  produced three negative gravity closures interpreted as buried calderas. The proposed repository itself lies within more than 2000 m of tuff on the eastern margin of one of these extinct calderas possibly the source of a 14.0-m.y.-old tuff; this caldera is one of several calderas at the south end of the Timber Mountain caldera complex.

Gravity modeling indicates that Yucca Mountain is underlain by 3500 m or more of tuff filling the southern edge of a gigantic depression in pre-volcanic rocks. This depression occupies as much as 1000 km<sup>2</sup>, embracing the entire volcanic mass surrounding Timber Mountain. An isostatic gravity residual anomaly of -20 mgal near Caliente, Nev. suggests that a similar caldera complex occurs near 37°30'N latitude just west of the Nevada-Utah border. The Pahranagat shear zone, a belt of shallow seismicity and discontinuous left-lateral surface faults about 65 km southwest of Caliente, coincides with a 20-mgal gravity gradient. This gradient and both caldera-related gravity lows lie along the southern border of a large negative Bouguer anomaly that becomes less pronounced after isostatic correction. The subdued isostatic anomaly suggests this southern borderline is the location of a regional change in crustal structure, possibly extending into the upper mantle.

T3-2-A-10

#### PRELIMINARY INVESTIGATION OF CRUSTAL STRUCTURE BENEATH THE VALLES CALDERA, NORTH-CENTRAL NEW MEXICO

Roger N. Felch (Dept. of Geosciences, Geophysics Program, Pennsylvania State Univ., University Park, Pa. 16802)  
Kenneth H. Olsen (Geophysics group, Los Alamos National Laboratory, Los Alamos, N.M., 87545)

Several seismograms were obtained through the Los Alamos National Laboratory short period seismic network. The network is centered in north-central New Mexico encompassing the Valles Caldera region. Events examined on the seismograms include local and regional mine blasts, teleseisms and low magnitude local earthquakes. Location of the local events indicates the caldera region is predominantly seismic.

Comparison of the seismic records from stations within the caldera region to those in the surrounding vicinity suggests the crustal structure underlying the two regions is different. For the same event, station records from the caldera region exhibit lower body wave amplitude (both P and S) and less energy in the higher frequency portion of the signal than station records from the vicinity around the caldera.

These results indicate the local seismic network is useful in identifying areas underlain by low rigidity material in the caldera region. However, additional seismic network or portable seismic stations are necessary to improve the spatial delineation of the anomalous region.

## V22C-173 1330H INVITED POSTER

Central Death Valley Volcanic Field, Eastern California; Tectonic Setting, Volcanic Stratigraphy, and Geochronology

L.A. WRIGHT, (Dept. of Geosciences, Pennsylvania State University, University Park, PA 16802)  
R.E. DRAKE, (Berkeley Geochronology Center, 2453 Ridge Rd., Berkeley, CA 94709)  
B.W. TROXEL, (Dept. of Geology, University of California, Davis, CA 95616)  
R.A. THOMPSON, (U.S.G.S., Denver, CO 80225)

Cenozoic volcanic and plutonic units of the Black Mountains and Greenwater Range, eastern California, define a 1600-km<sup>2</sup> rhombochasm between the terminations of the *en-echelon*, right-lateral, northwest-trending Furnace Creek and Sheephead fault zones. The volcanic pile overlies Late Proterozoic and Cambrian sedimentary rocks, Mesozoic(?) diorite and Cenozoic quartz monzonite plutons, and locally, Early Proterozoic rocks.

K-Ar age determinations indicate that Cenozoic igneous activity extended from about 14 Ma into Quaternary time. Normal faulting, contemporaneous with strike-slip faulting, has commonly tilted older volcanic units 80-90°; whereas, the younger units are horizontal or gently tilted.

The volcanic pile is typically 800-1200 m in observed thickness and composed of three dominantly silicic sequences, commonly separated by unconformities: (1) a lower sequence (14-10 Ma) of dacitic lava flows and air-fall tuffs, (2) a middle sequence (9-7 Ma) dominated by rhyolite lava flows and air-fall tuffs of the Shoshone volcanics, including pre-Shoshone andesite flows and rhyolite ash-flow tuffs, and (3) an upper sequence (7-5 Ma) of rhyolite lava flows and air-fall tuffs of the Greenwater volcanics. No caldera sources have been identified for any of the silicic tuff units.

Basaltic volcanism has occurred episodically during the past 9 m.y.; it culminated around 4 Ma, but has continued into Quaternary time (the most recent activity was 0.78 Ma). Basaltic rocks of the volcanic field appear to be petrologically similar to widespread coveal basalts of the southwest Nevada volcanic field.

## V22C-174 1330H POSTER

The Mid-Miocene Lake Mead Volcanic Field, Southern Nevada: Geochemical Constraints on Magmatic Evolution

SMITH, EUGENE I., Dept. Geoscience, University of Nevada, Las Vegas, NV 89154  
MILLS, JAMES G., Dept. Geology, Michigan State University, East Lansing, MI 48824

Volcanic rocks of the mid-Miocene (12-20 Ma) Lake Mead Volcanic field (LMVF) have calc-alkaline or alkali-calcic affinities, vary continuously in composition from andesite to dacite (basalt and rhyolite are present but rare), and form several stratovolcano complexes. Ash-flow sheets are associated with small caldera-like structural depressions at Hoover Dam, in the central McCullough Range and at Devil Peak in the southern Spring Range. In the Lake Mead area and to the south along the Colorado River, volcanic rocks are associated with cogenetic plutons.

Volcanic complexes in the LMVF form two major rock suites. Suite 1 (River Mountains and Hoover Dam volcanoes and the Wilson Ridge Pluton). Rocks of suite 1 are characterized by decreasing total rare-earth element (REE) content with increasing SiO<sub>2</sub>, and contain <2 ppm Ta. In the River Mountains there are four pulses of activity. Each began with the eruption of intermediate lavas (54-60% SiO<sub>2</sub>) and terminated with the emplacement of dacite domes and flows (65-69% SiO<sub>2</sub>). At Hoover Dam, an ash-flow tuff at the base of the section, displays reverse mineralogical and chemical zonation. SiO<sub>2</sub> varies from 66% (top) to 59% (base); biotite and hornblende increase in modal abundance upward and clinopyroxene and plagioclase increase downward. The upper part of the Hoover Dam section is composed of dacite flows and associated volcanoclastic rocks bounded above and below by flows of andesite (55% SiO<sub>2</sub>). Suite 2 (Volcanic sections in the northern Eldorado and McCullough Mountains and the Boulder City Pluton). Rocks of suite 2 vary in SiO<sub>2</sub> from 55% to 74%, show increasing total REE content with increasing SiO<sub>2</sub> and contain >5 ppm Ta.

## V22C-175 1330H POSTER

Remote Sensing Analysis of Southern Walker Lane

NANCY D. WALKER (Nevada Bureau of Mines and Geology, Reno, NV 89557) and David B. Stiemmons (Dept. of Geology, University of Nevada-Reno, Reno, NV 89557)  
H. L. MCKAGUE (Lawrence Livermore National Laboratories, Livermore, CA 94550)

A comprehensive analysis of Landsat Thematic Mapper imagery and geologic, topographic, and aeromagnetic maps demonstrates that the Walker Lane is a continuous feature through the southwestern Nevada volcanic field. A northwest pattern of lineaments is apparent in rock units older than 9.5 m.y. These lineaments correspond to sites of aligned preferential erosion and, at intersections with lineaments of different trends, may be northwest-trending vertical fractures and faults. The lineaments in volcanic rocks are thought to owe their origin to movement on northwest-trending structures in the

underlying Paleozoic basement.

A conspicuous lack of northwest-trending lineaments occurs in rock units younger than 9.5 m.y. The lack of these lineaments in young volcanic units may suggest that movement on the underlying structures ceased by the time of, or soon after, their deposition. Relative ages of the cessation of movement are provided by tuff units of the Black Mountain and Stonewall Mountain calderas. The 8.5 to 6.3 m.y. ages of the tuffs coincide with other evidence of a clockwise rotation of the stress regime at about that time. The lineament distribution therefore suggests cessation of movement along northwest-trending structures which may be related to a change in the orientation of the stress regime.

## V22C-176 1330H INVITED POSTER

Petrology and Geochemistry of Peralkaline Lava Flows and Tuffs, Silent Canyon Caldera, Southwest Nevada Volcanic Field

DAVID A. SAWYER, K.A. SARGENT  
U.S. Geological Survey, MS 913, Denver, CO 80225

The Silent Canyon caldera is a buried upper Miocene center of peralkaline affinity. Its location has been corroborated by geophysical data and more than 50 drill holes. The Tub Spring and Grouse Canyon Members of the Belted Range Tuff are the two widespread ash-flow sheets erupted from the Silent Canyon volcanic center (volumes of 60-100 km<sup>3</sup> and 200 km<sup>3</sup>, respectively). The eruption of these tuffs was preceded by rhyolite volcanic domes (Split Ridge and Quarter Dome), and was followed by lava flows and tuffs of Saucer Mesa (extracaldera), and Deadhorse Flat (intracaldera). Total subsidence on the Grouse Canyon Member within the caldera is 1525-2135 m.

Peralkaline tuffs and flows range from 65 to 77% SiO<sub>2</sub>, and have *agapitic* indices of less than 1.26. The most mafic compositions are pre- and post-caldera trachytes (65-69% SiO<sub>2</sub>). The Tub Spring Member is a relatively unzoned high-silica comendite, whereas the Grouse Canyon Tuff is strongly zoned (70-75 percent SiO<sub>2</sub>) in major- and trace-element composition. The volumetrically dominant precaldera flows are high-silica rhyolites, whereas post-collapse flows are petrologically diverse, ranging from trachyte through high-silica rhyolite. Rocks at Silent Canyon share a common petrologic evolution from trachyte to low-silica rhyolite; at more than 74% SiO<sub>2</sub>, a marked split in differentiation trends exists between the more peralkaline comendites (middle and lower tuffs of the Grouse Canyon Member and Split Ridge flows) that approach pantelleritic compositions and the less peralkaline comendites (Tub Spring Member and Quarter Dome, Saucer Mesa, and Deadhorse Flat flow rocks). Compared with peralkaline rocks worldwide, the Silent Canyon magmas were lower in Ba, Y, Nb, Th, and U and higher in Rb, Mo, and P/C1. Decoupling of trace-element variations from major-element chemical trends underscores the importance of volatile complexing in peralkaline petrogenesis.

## V22C-177 1330H INVITED POSTER

Geochemistry of Glassy Pumices from the Timber Mountain Tuff, Southwestern Nevada

JAMES G. MILLS, JR.  
TIMOTHY P. ROSE (Both at: Department of Geological Sciences, Michigan State University, East Lansing, MI 48824-1115)  
(Sponsor: T. A. Vogel)

The Rainier Mesa (RM) and Ammonia Tanks (AT) Members of the Timber Mountain Tuff each contain large variations in major and trace element compositions. Felsic, silica-rich pumice are phenocryst poor (2-5%; Pl, Or, Qtz, +/- Bio) while mafic pumice are phenocryst rich (20-35%; Pl, Bio, +/- Or, +/- Qtz). Pumice types in both tuffs are generally similar in lithology. Compositionally banded pumice are rare in the top of the RM, but common throughout the AT. Pumice compositions, intermediate to the end-members are present in both ash-flow sheets.

Member	%SiO <sub>2</sub>	%FeO	%MgO	Rb(ppm)	Sr(ppm)
Rainier Mesa	63.9-78.1	0.4-3.5	0-1.4	121-282	6-824
Ammonia Tanks	63.8-78.1	0.7-3.3	0-1.7	87-246	116-801

The RM has only high-silica pumices at the base, but a large compositional range among pumices at the top. The AT, however, has a large chemical variation among pumice types at the base and top of the ash-flow sheet. A probable comagmatic origin for the two tuffs is indicated by similar variations in major and trace elements and by previous field studies.

The RM magma may have been more evolved than the AT magma based on lower concentrations of La (137 vs. 170 ppm), Zr (526 vs. 801 ppm) and a relative depletion in Ba of 0.6x.

The presence of large chemical variations among pumices at the top of the RM and throughout the AT, are consistent with theoretical models for magma withdrawal from a zoned and/or layered magma chamber.

## V22C-178 1330H POSTER

The Mid-Miocene Wilson Ridge Pluton: a Subvolcanic Intrusion in the Lake Mead Region, Arizona and Nevada

FEUERBACH, DANIEL L., and SMITH, EUGENE I., Dept. Geoscience, University of Nevada, Las Vegas, NV 89154.

The mid-Miocene Wilson Ridge Pluton (WRP) in northwestern Arizona is a subvolcanic intrusion related to volcanic centers in the River Mountains (west of Lake Mead) and at Hoover Dam. Soon after emplacement, the volcanic-plutonic complex was cut by west-dipping detachment faults and upper levels of the pluton including its volcanic cover were transported as far as 20 km to the west. The pluton is composed of fine- to coarse-grained biotite-sphene bearing monzonite, quartz monzonite and granite. Biotite-lamprophyre, basalt, dacite, and granite porphyry dikes intrude the pluton.

The SiO<sub>2</sub> content of the WRP varies between 57% and 74%. Felsic dikes are highly evolved (up to 77% SiO<sub>2</sub>). One dike is zoned with a margin of diorite (55% SiO<sub>2</sub>) and a quartz monzonite core (67% SiO<sub>2</sub>). The pluton is characterized by low Ta (<2 ppm) and by decreasing total REE with increasing SiO<sub>2</sub>. The variety of rock types may be explained by models involving hornblende-biotite-feldspar-sphene dominated fractional crystallization. Sr isotope ratios (0.709) and trace and REE element ratios suggest that the Wilson Ridge magma was derived by partial melting of pyroxene granulite in the lower crust.

The WRP is correlated to its detached volcanic cover on the basis of (1) mineralogical similarities between fine-grained phases of the pluton and felsic volcanic rocks, (2) similar trends of decreasing REE content with increasing SiO<sub>2</sub> for volcanic and plutonic rocks, (3) low Ta values (<2 ppm), and (4) agreement with independent reconstructions based on the structural geometry of the Lake Mead area. After the major phase of eruption, the Wilson Ridge magma reservoir continued to evolve. As a result, evolved rocks of the pluton are higher in SiO<sub>2</sub> (72%-77%) and lower in total REE than evolved rocks of the cogenetic volcanic pile (67%-72% SiO<sub>2</sub>).

## V22C-138 1330H POSTER

Structural Implications of an Isostatic Residual Gravity Map of the Nevada Test Site, Nevada

R. H. Harris, H. W. Oliver (Both at: U.S. Geological Survey, 345 Middlefield Road, Menlo Park, CA 94025)  
D. L. Healey (U.S. Geological Survey, Denver, CO 80225)

Gravity anomalies at the Nevada Test Site (NTS) were investigated to determine the subsurface structural setting of volcanic terrane in the area. Bouguer and isostatic residual gravity maps of the NTS have been compiled with a 2-mgal contour interval at a scale of 1:100,000. The new maps are controlled by 14,753 stations and have been reduced assuming a Bouguer reduction density of 2.67 g/cm<sup>3</sup>. The regional isostatic field removed from the Bouguer map was computed assuming an airy model for isostatic compensation of topographic loads. On the basis of seismic refraction data this model assumes a crustal thickness of 25 km, a density of 2.67 g/cm<sup>3</sup>, and a density contrast across the base of the model crust of 0.4 g/cm<sup>3</sup>. The isostatic map shows a range of residual gravity values from -65 mgal over Silent Canyon caldera to +14 mgal over Bare Mountain. Major gravity lows occur over the Timber Mountain caldera moat (-42 mgal), Yucca Mountain (-38 mgal) and Emigrant Valley (-40 mgal). Significant highs of +6 to +10 mgal are associated with Paleozoic argillites and carbonates. The gravity characteristics of eight nested calderas in the southwestern Nevada volcanic field are very diverse. In contrast to the major low over the nonresurgent Silent Canyon caldera, a local gravity high of about 9 mgal occurs over the resurgent dome of Timber Mountain caldera, whereas Oasis Valley and Sleeping Butte calderas are characterized by gravity gradients with lows to the east. The gravity low over Silent Canyon caldera extends southward into the northern part of the younger Timber Mountain caldera, as originally observed by M.F. Kane, suggesting that the Silent Canyon collapse extends beneath the Timber Mountain volcanic sequence. To the south of Timber Mountain, a local residual gravity low of about 30 mgal occurs over Crater Flat, a suspected caldera that may extend partly under Yucca Mountain. Interpretation of the low is complicated by a regional increase of residual gravity to the west over pre-Tertiary bedrock, consistent with a model of an east-dipping detachment fault under the Crater Flat-Yucca Mountain area.

## Magma Transport and Convection I

CA 106 Wed AM  
Presider, F. Richter  
Univ of Chicago  
P. J. Wyllie  
Caltech

## V31-01 0845H

The Driving Force for Melt Segregation

NEILL M. RIBE (Dept. of Geology and Geophysics, Yale Univ., P.O. Box 6666, New Haven, CT 06511)

Segregation of melt from a partially molten source can be driven either by the buoyancy

and the locations of input data, a prior estimate of the variogram allows evaluation of the effectiveness of additional drill holes in reducing the kriging variance in advance of drilling those holes. Comparison of the estimated grid of values with the values at all points of the synthetic initial data set in this example demonstrates of the accuracy of the prediction technique.

**H12A-15 1300 H POSTER**

Determination of elastic and fluid flow properties from the response of wells to air pressure

Stuart Rolstaczer (U.S. Geological Survey, Menlo Park, CA 94025)

The water level in a well is often sensitive to air pressure changes. The magnitude and character of this response is governed by: the well radius, the lateral diffusivity of the aquifer, the vertical diffusivity of the saturated zone overlying the aquifer, the vertical air diffusivity of the unsaturated zone and the thicknesses of the overlying saturated and unsaturated zones. These elements can be combined into four dimensionless parameters which govern the phase and attenuation of the response. In many cases, the response of a well to air pressure can be broken up into a high frequency and a low frequency response. The high frequency response is governed by the well radius and lateral diffusivity of the aquifer. The low frequency response is governed by the vertical air diffusivity and thickness of the unsaturated zone and the vertical hydraulic diffusivity and thickness of the saturated material above the aquifer. When spectrally deconvoluted, the response of water wells to air pressure can be fit to a theoretical linear model to yield estimates of the key dimensionless parameters. If the well radius, saturated and unsaturated thicknesses of the region above the aquifer as well as the aquifer thickness are known, it is possible to make estimates of, or place bounds on, the hydraulic conductivity and specific storage of the aquifer, the vertical air diffusivity of the unsaturated zone and the composite vertical hydraulic diffusivity of the overlying saturated materials. Application of this technique to long term barographs and well hydrographs indicates that these estimates are physically reasonable and, when comparison is possible, agree well with other measurements.

**H12A-16 1300 H POSTER**

GEOPHYSICS OF SUPRATIDAL AND TERRESTRIAL PERMAFROST AT KANGIQSUALUJLUJQ, CANADA.

MAURICE-K. SEGUIN, M. ALLARD, E. GAHE and R. LEVESQUE  
Centre d'études nordiques, Université Laval, Québec G1K 7P4.

The area investigated (355 km<sup>2</sup>) is located in the southeastern sector of Ungava Bay (latitude: 58°30'N and longitude: 65°50'W). The Quaternary deposits (mainly till and marine deposits) overlie the crystalline bedrock of Precambrian age. Three types of periglacial morphologies in four different regions are discussed: 1) cryogenic mounds, 2) palisade plateaus and 3) peat plateaus. Geomorphology, surface and down-the-hole geophysics as well as water jet drilling allowed the determination of lateral and vertical extent of discontinuous permafrost. Electrical resistivity, electromagnetism, induced polarization, self potential, refraction seismic and geothermal methods were used. In cryogenic mounds and palisade plateaus, permafrost covers 11-15% of the area, and in peat plateaus 80%. In peat and palisade plateaus, the mean permafrost thickness is 8 m; it is 6 and 22 m for cryogenic mounds in supratidal and terrestrial environments respectively. A correlation of the morphometric parameters of the permafrost mounds (length, width, elevation, etc...) with their thickness allows a prediction of this thickness with a relative degree of certainty. Ground ice is lenticular in clayey silt and intergranular in sand and gravel. A model of evolution of permafrost in cryogenic mounds is presented; this model takes into account the thickness of permafrost, elevation of the mounds, isostatic rebound and dendrochronologic results.

**H12A-17 1300 H POSTER**

Discrete Analysis For Generating Second-Order Stationary Random Fields In Three-Dimensions

S.E. Silliman (Dept. of Civil Engineering, The University of Notre Dame, Notre Dame, IN 46556).  
A.L. Wright (Dept. of Mathematics, The University of Arizona, Tucson, AZ 85721)

Several techniques (e.g. turning bands and sampling from a spectrum) have been introduced for generating second-order stationary fields which reproduce the

first two moments of a parent distribution. One common limitation of these techniques is their restriction to consideration of normally distributed random variables. In this paper, a technique (termed Discrete Analysis, or DA) is introduced for generating second-order stationary fields without requiring an assumption of normality. DA is based on separating the univariate distribution and the covariance into two, independent generation steps. The covariance is modeled as a 0/1 process in which the values of the random variable at two points in space are randomly chosen to be either identical or independent; this choice is based on a probability structure dictated by the form of the covariance. Simulation results show that on average over a large number of simulations, the first and second order statistics generated by DA accurately reproduce the first two moments of the parent population. Results of an ongoing comparison between one version of discrete analysis and the turning bands method are presented.

**H12A-18 1300 H POSTER**

The Role of Heterogeneous Hydraulic Conductivity in Calculation of Subsurface Discharge from an Upland Catchment

FREDERICK J. TENBUS and GEORGE M. HORNBERGER (both at Dept. of Environmental Science, University of Virginia, Charlottesville, VA 22903)

The interactions between a stream and the alluvial infill in an upland catchment can affect the hydrological and hydrochemical budgets of the catchment. These flow processes and interactions are influenced by heterogeneity in hydraulic conductivity. The effect of heterogeneity on subsurface discharge calculations was examined in an upland catchment in Virginia. The alluvium at the catchment is about 100 m wide near the mouth, and it supports a permanent water table. The dimensions of the alluvium were determined with geophysics, and heterogeneity in hydraulic conductivity was quantified with infiltration testing. A model calculated subsurface discharge from the catchment using various realizations of the hydraulic conductivity array inferred from the infiltration tests. Results show that average hydraulic conductivity is more important than spatial variation in discharge calculation, but it may be impossible to determine average K in alluvium without quantifying heterogeneity.

**H12A-19 1300 H POSTER P**

Quantifying Spatial Variability in a Carbonate Aquifer

JOHN E. NEVILL, TIMOTHY M. LUTZ and ROBERT GIEGEGACK (all at: Geology Department, University of Pennsylvania Philadelphia, PA 19104)

Quantifying the spatial distribution and orientations of fractures and bedding surfaces in carbonate-rock outcrops provides valuable information on groundwater flow paths. We consider the spatial distribution of solution features (sinkholes) as sources of additional information. The sinkholes are more widely distributed than are fractures measured at distinct outcrop locations; sinkhole distribution therefore provides information that might be more appropriate for modeling groundwater flow. Our data consist of orientation measurements of fractures and bedding surfaces and plots of sinkhole locations from an area of approximately 25 km<sup>2</sup> underlain by Cambro-Ordovician carbonate rocks in Upper Merion Township, PA. The statistical method developed by Lutz (JGR 91, 421-434, 1986) was used to determine the extent to which features with linear trends can be related to the locations of sinkholes.

Significant control was indicated in each of several subareas. The trends of linear features deduced from the analysis of sinkholes vary among the subareas but are consistent with the orientations of the dominant fractures within each subarea. In the eastern portion of the area, WNW fractures are consistent with alignment of sinkholes along WNW trends. In the western portion, WNW fractures are virtually absent and there is no evidence for WNW trends in sinkhole distribution. The most consistent trend deduced from sinkhole locations is parallel to bedding surfaces (ENE).

The approach presented here for quantifying the spatial variability of fractures and bedding surfaces allows one to acquire field data in carbonate terrain characterized by minimum bedrock exposure. The bedding surface, fracture, and sinkhole-distribution data indicate that the aquifer represented by these rocks is particularly prone to solution enhancement of groundwater-flow pathways in an ENE direction (parallel to strike), and could therefore be more transmissive in that direction. This conclusion is supported by a water budget study that indicates that water migrates efficiently through the aquifer, along pathways that trend ENE, from the Schuykill River to a major regional supply reservoir 1.6 miles west of the River.

**H12A-20 1300 H POSTER**

Use of Drillers' Logs and Geophysical Surveys to Define the Hydrogeologic Framework of the Amargosa Desert, Southern Nevada

John S. Czarnecki  
William J. Outfield  
(Both at the U.S. Geological Survey, Denver, Colorado 80225)

The Amargosa Desert, in the Basin and Range province of southern Nevada, is hydraulically downgradient from Yucca Mountain, the site of a potential repository for high-level nuclear waste. Ground-water flow paths and flow rates beneath the Amargosa Desert are controlled in part by the total saturated thickness and the hydraulic properties of basin-fill alluvial sediments. As part of a study to estimate ground-water velocities in this area, drillers' logs of water wells completed in alluvium were analyzed, and ratios of the percentage of coarse- to fine-grained sediments were calculated for each of these logs. These ratios were contoured using a universal-kriging routine to interpolate values. For comparison, results from a vertical electrical sounding (VES) survey also were contoured. The VES results were obtained from individual depth-to-resistivity profiles, from which the average resistivity of the total depth, the resistivity of the upper 75 meters, and the estimated depth to Paleozoic (?) basement rocks were obtained. The distribution and variations in average resistivity of the total depth agreed reasonably well with the distribution of variations in regional gravity. Patterns of contours of the resistivity of the upper 75 meters of alluvium were similar to patterns of regional contours of depths to the water table in the area. Major highs and lows of the gravity-measurement contours coincided with the highs and lows of the ratios of the percentage of coarse to fine sediments. The lows probably correspond to the presence of lacustrine, eolian, or marsh deposits, that may act as barriers to ground-water flow. Contours of the estimated depth to Paleozoic basement rocks indicate depths as great as 1,000 meters, and appear to agree with recent seismic-refraction survey data.

**Field Approaches and Measurement Techniques for Quantifying Spatial Variability in Porous Media III (H12B)**  
Room 317 Mon PM  
Presider, F. J. Molz  
Auburn Univ

**H12B-01 1500 H**

Chemical Heterogeneity of Groundwater

MORDECKAI MAGARITZ (Isotope Dept., Weizmann Institute of Science, Rehovot 76100, Israel).  
DANIEL ROMEN (Isotope Dept., Weizmann Institute of Science, and Research Dept., Geological Service, Water Commission, Jerusalem 91063, Israel).

Large spatial variability was reported for hydrological parameters of soil and aquifers as a result of sedimentological, diagenetic and tectonic processes. There is a general assumption that the fluid phase chemistry in aquifers, at least on a fine scale, is rather homogeneous. A multilayer dialysis cell device was used to obtain detailed chemical profiles of upper water layers (up to depth of 2.5 m) in aquifers. One set of samples was taken from the Coastal Plain aquifer of Israel under a cultivated field irrigated by treated sewage and the second from a forest region in northeast Netherlands. In both regions large variations were observed in the concentration of Cl<sup>-</sup>, NO<sub>3</sub><sup>-</sup> and SO<sub>4</sub><sup>2-</sup> between samples that were vertically separated by as little as 3 cm. Even larger variations were observed in samples taken within one month in the same water horizon in the same well.

These data give for the first time a clear view of the chemical fine structure of groundwater. Such observations provide new insights into mechanisms of contamination of an aquifer by surface inputs and raises the question of the validity of groundwater quality data based on single samples. Noneven obtained.

**H12B-02 1515 H INVITED**

A Natural-Gradient Experiment on Solute Transport in a Sand Aquifer: Spatial Variability of Hydraulic Conductivity and its Role in the Dispersion Process

E.A. Sudicky (Institute for Groundwater Research, University of Waterloo, Waterloo, Ontario, N2L 3G1)

The spatial variability of hydraulic conductivity at the site of a long-term tracer test performed in the Borden aquifer was examined in great detail by conducting permeability measurements on a series of

cores from other two cross-conductivity horizons; aquifer lenses of Estimation structure indicate variance correlation. A value calculated three-d by vertical statistical in Dagan predicted transverse vertical essential in the analysis independent-Borden a of injection promise transport aquifers variability.

**H12B-03**  
Theoretic  
DAVID J. (Larry W. J. (both w. The Univ. 78712) (Sponso

Generat condition requires, can be o developed a large 5%, non- in this of the ca. Permeab corrected We give of the flow of valida data. between range of at the 10 turbulenc accounted

**H12B-04**  
Measureme of hetero Fully Ser

KENNETH R. LYNN W. G

Vertical small dia sensitive measureme for a set thickness in the bu calculati zates pe conducti head disc At the st Columbus been made 25-30 fo measurem of the w conducti hydroavi within a of aquit solute to represent autocovar conducti measurem autocovar

dipolar. However, the field was dominated by low order zonals. Such transition field geometries give paleomagnetic records of reversals, which always include high inclinations, approaching either +ve or -ve 90°. Subsequently, when transition records without such high inclination were found the idea of the dominance of low order zonals appeared to be discredited. We show that if the low order zonals are combined with a drifting non-dipole field, similar to that seen at present, most of the features of reversal transitions can be simulated. The presence, or absence, of the very high inclinations depends upon the latitude and longitude of the observation site. We therefore conclude that low order zonals may indeed dominate transition fields, but they are accompanied by some form of drifting non-dipole field.

**GP11-110 0830H POSTER**  
**Dynamics and Energetics of Earth's Core During a Geomagnetic Reversal**

**S.J. PEARCE**  
 E. H. LEVY (both at Lunar and Planetary Laboratory, University of Arizona, Tucson, AZ 85721)

Estimates of the energy budget in Earth's core suggest that the energy available to power the geomagnetic dynamo does not greatly exceed that needed for usual regeneration of the field. During a geomagnetic reversal, the energy supply problem seems to be exacerbated because the entire field must be reversed and reconstituted in only a few thousand years. Thus, on its face, the power delivered to the geomagnetic field seems to be substantially more than an order of magnitude greater during a geomagnetic reversal than during the normal dynamo regeneration. In this paper we discuss core dynamics and large-scale motions during a geomagnetic reversal and show that the energy stored in the toroidal field is essentially preserved through the reversal event. Thus the energy needed to power a geomagnetic reversal is not larger than the energy needed for the usual regeneration processes.

**GP11-111 0830H POSTER**  
**Another Geodynamo Model**

**WILLIAM M. ADAMS, AUGUSTINE S. FURUMOTO, JACK McMILLAN and YUKO OGUCHI** (Hawaii Institute of Geophysics, 2525 Correa Road, Honolulu, HI 96822)

A novel geodynamo model is proposed. At the evolutionary stage of liquid core-solid mantle; (1) outer core cooling creates gravitational differentiation; (2) each sinking conductive nodule transports angular momentum and perhaps any ambient internal magnetic field towards the center; (3) the inner solid core formed from the accreting nodules rotates faster than the outer liquid core; (4) using the simple  $\vec{v} \times \vec{r}$  approach (Melchior, 1986, pg. 142) approach, the toroidal and poloidal electric and magnetic fields are potentially regenerative. This model removes the usual assumption of an external ambient magnetic field; nor does it require recourse to the more complicated mechanisms of turbulence and/or boundary layers. While these latter features are both intriguing and existent, our model of minimal complexity (i.e. maximal aesthetics) is proposed for attaining description, tutorial, and prescriptive objectives.

Melchior, P., "The Physics of the Earth's Core," Pergamon Press, 1986.

**GP11-112 0830H POSTER**  
**Secular Variation of Magnetic Observatory Annual Means**

**MALCOLM G. McLEOD** (Naval Ocean Research and Development Activity, NSTL, MS 39529)

The spatial and temporal variation of the geomagnetic field component annual means has been analyzed. The data used in this study consist of the annual means of the vector magnetic field components measured at over one hundred magnetic observatories widely distributed about the Earth. The data that have been analyzed are for the time interval 1970-1980.

Spherical harmonic models of the mean magnetic field have been computed for each year within the time interval indicated. Coefficients corresponding to both internal and external sources were included in the models. Spherical harmonic models have also been computed for the first and second time differences of the field using first and second time differences of the annual means as input data. Filtered versions of these models have also been computed.

External current systems are found to be responsible for a significant portion of the first and second time differences of the annual means of the geomagnetic field. While most of the effect of the external current systems can be modeled by degree one spherical harmonics, higher degree spherical harmonics are also important for modeling the field due to external sources. The time variation of the external sources is correlated with the sunspot cycle and includes harmonics of the sunspot cycle.

**Rock Magnetic Applications to Tectonic Studies (GP12)**  
 Room 308/310 Mon PM  
 Presiders, J. Geissman  
 Univ of New Mexico  
 S. Cisowski  
 Univ of California, B

**GP12-01 1330H**  
**Identification of magnetic carriers in the Monterey Formation.**

**M.Hart** and **M.Fuller** (Department of Geological Sciences, University of California, Santa Barbara, CA. 93106.)

Two well correlated stratigraphic sections, which are exposed in wave cut terraces about 4 kms apart on the coast in Santa Barbara County, have been sampled to identify the magnetic carriers in a variety of rock types. In certain dolomites, which show a primary direction of magnetization, detrital magnetite has been identified using TEM. The same dolomite approximately 30m along strike shows a secondary magnetization direction. Comparison of NRM:IRMs ratios revealed that the secondary magnetization process was more efficient than the primary by a factor of about 5 and has apparently overprinted any primary detrital remanence. Detrital magnetite is not seen in the various lithologies which carry secondary magnetization, including dolomites, siliceous mudstones, and organic phosphatic shales. A primary direction was also seen in an early sulphide nodule. We suspect that the magnetization in this case is carried by an authigenic phase derived from a tetragonal form of FeS. Dolomite fracture fill associated with hydrocarbon migration has weak but measurable natural remanent magnetization consistent with late stage formation. The diagenetic history of these various rock types accounts for the observed natural remanent magnetization.

**GP12-02 1345H INVITED**  
**Remagnetization in the Monterey and Siskyou Formations**

**S.M. CISOWSKI, M. HART, M. FULLER** (Dept. of Geological Sciences, University of California, Santa Barbara, CA)

Combustion metamorphism (CM) in bituminous shales generally produces a single component of magnetization which accurately reflects the direction of magnetization during natural burning. Because of the high temperatures reached during combustion, it should be possible to obtain absolute age determinations, via K-Ar and thermoluminescence methods, relating to the remagnetized field directions associated with the affected rocks.

Paleomagnetic samples from CM zones within the Monterey and Siskyou Formations of Southern California give high precision, unambiguous field vector directions, particularly in contrast to the unmetamorphosed rock. Although directional variation between most of the sampled sites can be explained in terms of secular variation of the present normal dipole field, several sites seem to record progressive clockwise rotations, up to 55°, which occurred during and since the time of burning. These local rotations may be related to left lateral strike slip faulting in the immediate area.

A considerable age of burning is indicated by the reversed magnetization at one CM zone (Casimalia), and a K/Ar age date of 0.8 my. Field vectors from another CM site (Vandenberg AFB) match the present field inclinations only after structural correction. This indicates that the burning and resulting remagnetization occurred before formation of a major anticlinal structure. In this case age dating of the CM zone would provide an upper limit on local folding events.

Paleomagnetic results from CM zones may also help in interpreting isothermal remagnetization directions in these same formations, which result from diagenesis and hydrocarbon migration.

**GP12-03 1400H**  
**Magnetic Property Variations and The Origin of**

**Paleomagnetic Carriers in an Ash-Flow Sheet at Yucca Mountain, Nevada**

**J.C. ROSENBAUM** (U.S. Geol. Survey, Denver, CO 80225)  
**C.M. SCHLINGER** (Univ. of Utah, Salt Lake City, UT 84112)

The magnitude of natural remanent magnetization (NRM) and magnetic susceptibility (K) vary systematically, by over an order of magnitude, through a 115-m-thick section of a Miocene rhyolitic ash-flow sheet, the Tiva Canyon Member of the Paintbrush Tuff, at Yucca Mountain, Nevada. The variations in NRM and K are related to changes in mineralogy, quantity, and grain size of the magnetic phases. A cubic phase (magnetite or maghemite) dominates the magnetic properties throughout the unit (based on IRM acquisition,  $J_s$ -T measurements, and transmission electron microscope (TEM) study) despite the abundance of hematite in parts of the sheet.  $J_s$  was used to estimate the relative quantities of

the cubic phase, correlates highly ( $r=0.9$ ) with K but not with NRM. Instead, NRM depends strongly on grain size. NRM increases upwards from the base of the ash-flow sheet by an order of magnitude, reaches a maximum in a thin vitrophyre 9 m above the base, and then decreases by a factor of 6 in the next 10 m. Magnetic grain sizes increase upwards through this 19-m interval as indicated by changes in coercivity of remanence, median destructive induction, frequency dependence of magnetic susceptibility, and decay rate of SIRM, as well as by TEM observations. Near the base a significant fraction of superparamagnetic grains accounts for relatively low NRM. An upward increase in grain size produces a high proportion of stable single-domain grains and high NRM; further increase in grain size produces pseudosingle and multidomain grains that are responsible for lower NRM in the interior of the sheet. The increase in grain size of the magnetic minerals away from the quenched base of the ash-flow sheet is consistent with the origin of these microcrystals by postemplacement growth from the volcanic glass.

**GP12-04 1415H**

**Paleomagnetic Carriers in an Ash-Flow Sheet at Yucca Mountain, Nevada: TEM Study of Fe-Oxide Microcrystals in Vitric and Devitrified Samples.**

**C.M. SCHLINGER** (Univ. of Utah, Salt Lake City, UT 84112)  
**D.R. VEBLEN** (Johns Hopkins Univ., Baltimore, MD 21218)  
**J.C. ROSENBAUM** (U.S. Geol. Survey, Denver, CO 80225)

We have used transmission electron microscopy (TEM) to image and analyze Fe-oxide microcrystals in three samples from the Miocene aged Tiva Canyon Member of the Paintbrush Tuff. The samples were collected 3.8 m, 7.6 m, and 18.5 m above the base of a 115-m-thick section of the ash-flow sheet at Yucca Mountain, Nevada. The mineralogy and chemistry of the microcrystals have been determined using electron diffraction and analytical X-ray methods. The lowermost sample, which is nonwelded and vitric, contains uniformly distributed elongate microcrystals of cubic Fe-oxide ( $Fe_3O_4$  or  $\gamma-Fe_2O_3$ ) with typical dimensions of ~20 nm by ~140 nm. These microcrystals are tapered and commonly vermiform. Fe-oxide microcrystals in glass of the middle sample, a densely welded vitrophyre, are also cubic; however, in contrast to those in the lowermost sample, these microcrystals are much larger (typical dimensions are ~50 nm by ~700 nm), are lath-shaped, and are clustered. The uppermost sample is a densely welded, mostly devitrified tuff. Analyzed Fe-oxide microcrystals are manganeseiferous hematite, have typical dimensions of ~120 nm by ~800 nm, and are distributed nonuniformly in the sample. The increase in mean dimension of these crystals, moving upward from the quickly cooled vitric margin to the more slowly cooled devitrified interior, is consistent with nucleation and growth of the microcrystals from volcanic glass at high temperatures (500°-700°C) after emplacement of the sheet. Many of the observed microcrystals are about the size of stable single-domain grains. The TEM observations are consistent with systematic variations in magnetic property data from throughout the sheet. We interpret these variations to reflect changes in size and quantity of the fine-grained magnetic constituents with vertical position.

**GP12-05 1430H**

**Thermoviscous/Thermochemical Partial Remagnetization of Late Paleozoic Strata, VC-1 Corehole, Valles Caldera, New Mexico**

**John Wm. Geissman** (Department of Geology, University of New Mexico, Albuquerque, New Mexico 87131)

Paleomagnetic and rock magnetic data from azimuthally unoriented core samples, collected at approximately 3 m intervals and in greater detail over selected areas, from the VC-1 CSDP Experiment have prompted significant reinterpretations of the Quaternary volcanic section intersected and have aided in understanding the thermal regime within the late Paleozoic strata attending fluid circulation and mineral deposition during and after development of the Quaternary Toledo and Valles calderas. The Permian Abo Formation, Pennsylvanian to earliest Permian Madera Limestone, and Pennsylvanian Sandia Formation typically contain a moderate pos. incl. RM component (e.g., Madera Lst.:  $I=58.4^\circ, \alpha_{95}=2.8^\circ, k=33, N=101$  samples); when residing in magnetite it is usually unblocked by 350°C; when carried by hematite, it is unblocked by 550°C. A moderate neg. incl. RM (e.g., Madera Lst.:  $I=173.1^\circ, I_s=-46.6^\circ, k=18, \alpha_{95}=5.5^\circ, N=36$  samples; assuming that the pos. incl. RM is N-seeking) is often isolated and removed at higher  $T_{ub}$ 's (up to 550° in magnetite-dominated and 600° in hematite-dominated lithologies). Where present, shallower incl. RM's (e.g., Madera Lst.:  $I=161.2^\circ, I_s=-9.8^\circ, k=34.5, \alpha_{95}=5.3^\circ, N=20$  samples) are removed over higher ranges of  $T_{ub}$ 's and these are suggested to be of late Paleozoic age. The pos. incl. RM's are in all likelihood VPTM's activated at near-present down-hole temperatures during the Brunhes and possibly within the last 10 ka. The neg. incl. RM's were activated at moderate (ca. 300°) temperatures between 1.45 and 0.97 Ma, attending and following the main stage of Valles Caldera development during the Matuyama. The inferred temperatures for thermal activation of the two magnetization agree with independent estimates of Quaternary thermal activity. The preservation of Matuyama age RM's in the Madera Lst. requires temperatures below 350° since 730 ka.

GP12-06

**Antisecropy - Perkins Plus Application**

**James E. Farr**  
 New Mexico  
 John Wm. Geissman  
 Christopher

As part of along a unit of NW Arizona and units Precambrian of the center down call of paleomagnetic N-12 sites. rocks just appears may lineation of Several sites NE margin of Max direct incline appears to be most current pluton, UT and rough the AMS fabric in Miocene initial pluton into but in this oriented NRM direction.

GP12-07

**Secondary Allowez**

**HUI LIN I**  
 Tech. I

Although thought component component units. component cobbles. Conglomerate. Volcanic magnetite all sites (CRM) callowing formed d similar the surr 1987, Ca producti sporadic 3) In si were dif towards, Indicati compon result i and magn sing d with, bu magnetit copper to CRM, magnetite northern. Greenst.

GP12-08

**Soft-S Late**

**D. Y. S**  
 of Ge Calif  
 N. H. R  
 physi  
 N.H.S.V

Altho Precamb depos: glass: linox: the a have soft-lates (1) t: (2) t: and W deformat stone A mic the h (1977) of th.



ent limitation in the physics causes distortions and artifacts in the reconstructed tomographic image that can be mistaken for real seismic structures. To deal with the problem of reconstructing tomographic images from incomplete data we use a priori information to constrain the model parameters. The method is based on the theory of projections onto convex sets. It iteratively constrains model parameters both in the space and wavenumber domains. Useful constraints in the space domain are positivity constraint and constraint on the amplitude range of the model parameters. Constraint on the geometrical shape of the object being imaged can also be applied if it is approximately known a priori. In the wavenumber domain, the wavenumbers that are obtained from the limited data are conserved and constraint is applied on the energy of the extrapolated wavenumbers that are not contained in the data. We apply these methods to a 2-D travel time tomographic inversion of field data from a seismic cross-borehole experiment in crystalline rock [Wong et al., 1983]. This method can also be directly applied to seismic source tomography for data that satisfy the Fraunhofer approximation. We will demonstrate how distortions and artifacts in the tomographic image of the cross-borehole data are significantly reduced by applying the constraints and we will also discuss the limitations of this method.

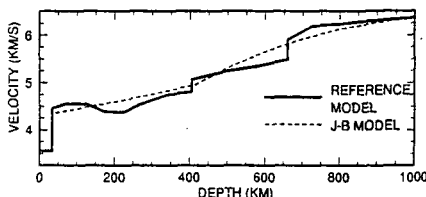
Wong J., P. Hurley and G.F. West (1983). GRL, 10, 686-689.

S41A-8 0830H POSTER

Upper Mantle Shear Velocity Structure Beneath Europe and the Mediterranean From ISC S Delays

Alet Zielhuis and Wim Spakman (Both at: Dept of Geophysics, University of Utrecht, P.O. Box 80.021, 3508 TA Utrecht, The Netherlands)

A fundamental problem in linearized delay time tomography is the choice of the reference model with respect to which the velocity perturbations are determined. We examined 80,000 S delays, reported by the International Seismological Centre, belonging to ray paths with turning points below Europe and the Mediterranean. The average value of the delay time data as a function of epicentral distance differs systematically from zero. This indicates that the average velocity structure beneath the area deviates systematically from the Jeffreys-Bullen (J-B) S model. We obtained a new 1 dimensional reference model by inversion of a travel time curve that was derived from the delay time data (Zielhuis et al., 1989, see figure). The presence of a low velocity zone and a "400-km" and a "670-km" discontinuity results in a more realistic ray geometry.



We present preliminary results from tomographic imaging of the upper mantle shear velocity structure beneath Europe and the Mediterranean using S delay time data corrected with respect to and ray paths calculated from the new model and we discuss associated problems.

Zielhuis, A., Spakman, W. and G. Nollet, *Ettore Majorana Int. Sc. Series, Physical Sciences*, Plenum Press, New York, 42, p. 333, 1989.

S41A-9 0830H POSTER

Dinobusting: Geophysical Diffraction Tomography in Exploration Paleontology

Alan Wilten (Energy Division, Oak Ridge National Laboratory, Oak Ridge, TN 37831-6045; 615-574-5805)  
Wendell C. King (U.S. Army Environmental Hygiene Activity-West, Aurora, CO 80045-5001; 303-361-8100)  
Jozef Sypniewski (Division of Engineering Technology, Wayne State University, Detroit, MI 48202; 313-577-8075)  
David D Gillette (Division of State History, 300 Rio Grande, Salt Lake City, UT 84092; 801-533-4563)  
J Wilson Bechtel and Peggy Bechtel (Both at: Southwest Paleontology Foundation, Inc., 314 Richmond SE, Albuquerque, NM 87106; 505-265-1376)

Geophysical methods are routinely applied to characterize subsurface conditions in support of resource exploration, foundation evaluation and hazardous waste site remediations. More recently, geophysics has been employed to characterize sites believed to be of archeological significance. While modern geophysical techniques are playing an ever-expanding role in a wide variety of applications, it has only been in the past several years that such techniques have had any impact on the century-old methods of paleontology.

For the most part, geophysics in paleontology has been limited to a single site at which the excavation of "seismosaurus", the longest dinosaur yet discovered, is underway. This paper describes the character of the site, the target supertitan sauropod dinosaur and the applications of geophysical diffraction tomography (GDT) a remote sensing technique of recent research interest, as an aid to the ongoing excavation. The GDT method is a generalization of the imaging algorithms used in CT scanners for diagnostic medicine, but implemented in a fixed measurement geometry and accounting for wave propagation phenomena. Two GDT field studies have been completed to date using both cross-borehole and offset vertical seismic profiling configurations. Results of these studies suggest that most, if not all, of the skeletal remains exist and are in near

articulation. While it is estimated that several more years are required to complete excavation, work to date has verified all results of the GDT surveys in the regions excavated.

S41A-10 0830H POSTER

Seismic-Refraction Study of Crustal Structure for Southern Great Basin, Nevada

P.S. Chang (Gallegos Research Group, under contract to the U.S. Geological Survey, Box 25046, MS 968, Denver Federal Center, Denver, CO 80225)

P-wave arrival times from nuclear tests in Nevada Test Site (NTS), Nevada, and chemical explosions near Bare Mountain, Nevada were used in this study. Fifty-five vertical-component stations in the southern Great Basin, Nevada (SGB) and southern California sampled this 300 x 400 km<sup>2</sup> region. Arrival times for P-waves from nuclear tests were scaled with a precision of 0.03 second. Plane horizontal layers were generated using these data in a least-squares algorithm. Results are as follows: (a) The first three layers have P-wave velocities of 3.80, 5.93, and 6.13 km/s, and thicknesses of 1.3, 2.3 and 20.1 km, respectively. Below the 6.13 km/s layer are two layers with P-wave velocities about 6.76 and 7.78 km/s; however, data are insufficient to determine their thicknesses. (b) No significant low-velocity zone (a layer with an area larger than 30 x 30 km<sup>2</sup> and thicker than 1.0 km inside NTS, or larger than 100 x 100 km<sup>2</sup> and thicker than 2.0 km outside NTS) exists at depths between 1.3 and 24 km. (c) A high-velocity region exists in the northeast region of the SGB network; this layer, having a P-wave velocity of 6.01 km/s, begins at a depth of about 1.05 km. (d) The layer with P-wave velocity of 5.64 km/s at Yucca Mountain is deeper than the layer with P-wave velocity of 5.93 km/s outside Yucca Mountain. (e) Comparison of station corrections of many stations for Pahute Mesa tests and Yucca Flat tests suggested that a high-velocity region about 15 x 15 km<sup>2</sup> lies inside NTS. Negative residuals will be contributed to the travel times if waves transgress this region. Velocity structures for these different paths and regions might be sources azimuthally dependent. (f) Some nuclear tests were relocated using this new model and station corrections; average location errors for the regional model and the new model were 1.2 km and 0.6 km, respectively, from the true locations.

S41A-11 0830H POSTER

Mapping an Overthrust Near the San Andreas Fault Using a Combination of Seismic Reflection Profiling, Ray Tracing and Gravity Modeling

Y. G. Li and Henyey, T. L. (Department of Geological Sciences, University of Southern California, Los Angeles, CA 90089)

Seismic and gravity data have been used to characterize a small buried overthrust structure discovered north of the San Andreas fault along COCORP Mojave line 1 (N-S 26 km) in southern California. Reprocessing of the COCORP reflection data generated a high resolution CDP section of the first 2 sec (TWTT). The CDP section provided a starting model for refinement of the image of the overthrust using ray tracing. Refraction and reflected refractions on the shot gathers were used to constrain the modeling and provide a refined image.

Gravity measurements were made at each shot point along the seismic line and along two short lines parallel to the major line 0.75 km and 3.2 km apart, respectively. Bouguer gravity profiles were computed. The refined image determined on the basis of the seismic data was used as input to 2 1/2D gravity modeling and a final structural interpretation of the overthrust was determined as the best fit to a combination of the seismic and gravity data.

The buried thrust dips northward with a ENE strike, consistent with sub-normal compression across the San Andreas fault. The overthrust portion of the basement was found to have a steep southward facing scarp abutting a small basin filled with low velocity, low density materials. Several lesser such structures were found elsewhere along the survey line, suggesting substantial regional N-S compression across the western Mojave block.

S41A-12 0830H POSTER

Crustal Structure of Northern England From High-Resolution Wide-Angle Seismic Data

T E West and R E Long (Both at: Dept. of Geological Sciences, University of Durham, South Road, Durham DH1 1LE, U.K.; 91-374-2510)

In June 1987, Durham University recorded on land the wide-angle seismic arrivals from airgun shots fired during the MOBIL (Measurements Over Basins to Image the Lithosphere) deep normal-incidence reflection profiling programme in the North Sea.

The resulting wide-angle records are of unique density and excellent quality but very complicated, showing many arrivals which were unresolved on previous wide-angle reflection/refraction experiments in this region. The data recorded in Northumberland particularly has been modelled using BEAMB7, Cervený's Gaussian Beam synthetic seismogram package, complemented by the reflectivity package, SYNSEI. The basic model which is emerging is that of a 30 km thick crust with a velocity jump at approx. 20 km depth, a steep velocity gradient within the lower crust and a high velocity layer 2 km thick at the base of the crust.

There is however strong lateral inhomogeneity giving rise to the complexity observed in the record sections. The wide-angle reflection from the Moho forms not a single arrival but a band of discontinuous, overlapping reflections, similar to what is seen by normal incidence profiles and termed 'the reflection Moho'. There is also a very high amplitude band of arrivals branching off the Moho reflection, exhibiting the travel time properties of a diffraction on some of the common station sections. This may be due to a step on the Moho or to a dipping reflector which disrupts it.

This dataset is not only exactly coincident with a normal-incidence reflection programme, but of equal resolution, thus enabling the extraction of a detailed crustal model from the two complementary techniques.

S41A-15 0830H INVITED POSTER

Structure of the Lower Crust Beneath the Midcontinent Rift from Inversion of Wide Angle Reflection Travel Times for Interface Position

A. M. TREHUB (College of Oceanography, Oregon State University, Corvallis, OR 97331)  
W. J. LUTTER and R. L. NOWACK (both at: Dept. of Earth and Atmos. Sci., Purdue University, West Lafayette, IN 47907)

Strong wide-angle reflections from the lower crust and Moho beneath the Midcontinent Rift in Lake Superior are observed in large aperture data recorded along GLIMPCE line A. We have inverted the travel-times of these reflections to determine the positions of lower crustal interfaces using the method of Lutter and Nowack (in press). Interfaces are parameterized using a one-dimensional spline where depths are specified at fixed horizontal node positions. A velocity model determined from an inversion of first-arrival travel-times for the same data set (Lutter et al., 1989) was used to define the velocity above the lower crustal interface. Resolution values greater than 0.1 indicate that the position of the lower crustal interface is well contained over the central 3/4 of the profile; it is located at approximately 23 km depth beneath both ends, at 34 km beneath the half-graben, and attains a maximum depth of about 45 km beneath the Isle Royale Fault Zone. The geologic significance of this interface, however, is uncertain because it may actually represent several different geological features that are not structurally continuous across the model. Resolution values of at least 0.7 indicate that the position of the Moho is well determined beneath the lake. It deepens abruptly from about 41-45 km beneath the southern shore of Lake Superior to about 57-61 km beneath the axis of the main rift half-graben; it then shallows gradually to about 51-55 km depth beneath the north part of the lake. This result confirms early reports of unusually thick crust beneath Lake Superior and generally agrees with results obtained from the GLIMPCE data using other analysis methods. The range of values cited reflects our present uncertainty in the lower crustal velocity (6.9-7.6 km/s). Limits on the velocity contrasts across both interfaces will be obtained from forward modeling of the amplitudes of the wide-angle reflections in order to help constrain the geologic significance of these boundaries.

S41A-14 0830H INVITED POSTER

Simultaneous Inversion for Focusing and Attenuation

R.L. NOWACK (Dept. of Earth and Atmos. Sci., Purdue University, West Lafayette, IN 47907)  
A.M. TREHUB (College of Oceanography, Oregon State University, Corvallis, OR 97331)

In this paper, a parameterized time-domain model for the inversion of seismic refraction and wide-angle reflection data is presented. Assuming a general Gabor wavelet and the slight attenuation model of Cervený and Frangé (1982), an analytic expression for the time-domain pulse using either the ray method or Gaussian beams can be obtained. The parameters of the seismic pulse include the amplitude of the envelope, the travel time and the average period. The travel time is dependent on the velocity model. The amplitude of the envelope is dependent on focusing from the velocity structure as well as attenuation from the Q structure. The average period of the pulse is dependent on the attenuation model. Sensitivity operators can be obtained from this seismic pulse model. Previous workers have inverted for Q structure using amplitudes corrected for focusing using a velocity model obtained from a previous travel time inversion. Alternatively, spectral ratios have been used to invert for Q structure. In the model presented here, the envelope amplitude and the average period from time-domain measurements can be used to iteratively invert for the Q structure and to update the velocity model. Seismic data from the 1986 Lake Superior GLIMPCE OBS experiment are used to test the method. Trade-offs between changes in the velocity model and changes in the attenuation model are analyzed and various approaches to measuring the observed parameters are discussed.

S41A-15 0830H POSTER

Reprocessing of Line RU-10, Offshore Southern Santa Maria Basin, California

C. NICHOLSON (Institute for Crustal Studies, University of California, Santa Barbara, CA 93106), C. SORLIEN, and B. P. LUYENDYK (also at Department of Geological Sciences, University of California at Santa Barbara, CA 93106)

An 80-km north-south seismic reflection profile extending from about 34°N46' to 34°N03' was shot off Point Arguello in November 1986 for Rice University (RU) as part of the EDGE program. Data from 180 channels sampled at 4 ms were recorded out to 16 s. The line extends from the southern Santa Maria Basin into the offshore region of the Western Transverse Ranges province. Initial processing by HARC reveals unambiguous returns from basin sediments, the top of the Franciscan Formation, as well as possible volcanics associated with San Miguel Island. Significant signal is generally present down